MINERAL DUST AEROSOLS OVER THE SAHARA: METEOROLOGICAL CONTROLS ON EMISSION AND TRANSPORT AND IMPLICATIONS FOR MODELING

Peter Knippertz[1] and Martin C. Todd[2]

[1] Atmospheric mineral dust has recently become an important research field in Earth system science because of its impacts on radiation, clouds, atmospheric dynamics and chemistry, air quality, and biogeochemical cycles. Studying and modeling dust emission and transport over the world's largest source region, the Sahara, is particularly challenging because of the complex meteorology and a very sparse observational network. Recent advances in satellite retrievals together with ground- and aircraft-based field campaigns have fostered our understanding of the spatiotemporal variability of the dust aerosol and its atmospheric drivers. We now have a more complete picture of the key processes in the atmosphere associated with dust emission. These cover a range of scales from (1) synoptic scale cyclones in the northern sector of the Sahara, harmattan surges and African easterly waves, through (2) low-level jets and cold pools of mesoscale convective systems (particularly over the Sahel), to (3) microscale dust devils and dusty plumes, each with its own pronounced diurnal and seasonal characteristics. This paper summarizes recent progress on monitoring and analyzing the dust distribution over the Sahara and discusses implications for numerical modeling. Among the key challenges for the future are a better quantification of the relative importance of single processes and a more realistic representation of the effects of the smaller-scale meteorological features in dust models. In particular, moist convection has been recognized as a major limitation to our understanding because of the inability of satellites to observe dust under clouds and the difficulties of numerical models to capture convective organization.

1. INTRODUCTION

[2] Atmospheric aerosols are an important component of the climate system by virtue of their direct radiative impacts, indirect effect on cloud properties, the semidirect effect of these on atmospheric dynamics [*Forster et al.*, 2007], and finally their role in global terrestrial and oceanic biogeochemical cycles [e.g., *Jickells et al.*, 2005; *Mahowald et al.*, 2010]. Of the aerosol species, mineral dust is the dominant type by mass [*Textor et al.*, 2006], yet many processes associated with atmospheric dust and the associated climate impacts are poorly understood. Uncertainty in the magnitude of radiative forcing from dust aerosols remains high, especially at the regional scale [*Uno et al.*, 2006; *Todd et al.*, 2008a]. Efforts to quantify these processes and their repre-

sentation in models are at the cutting edge of climate science and represent one of the major challenges for Earth system modeling. In addition, dust affects living conditions for humans through affecting air quality, aviation and road safety, and human health by fostering respiratory diseases and meningitis epidemics [*Molesworth et al.*, 2002]. As a result, there is increasing demand for dust storm forecasts.

[3] The Sahara Desert is by far the most important dust source globally [*Prospero et al.*, 2002; *Washington et al.*, 2003], as such there is a critical need to understand aerosol processes in this region. The Saharan atmosphere is particularly interesting as it is characterized by extreme features, notably (1) record high temperatures and the deepest planetary boundary layer (PBL) on Earth reaching up to 5–6 km above ground [*Gamo*, 1996]; (2) very high aerosol optical thickness (AOT) during most of the year (Figure 1); and (3) the summertime Saharan heat low (SHL), which colocates with aerosol maxima and is pivotal for the West

---

[1]School of Earth and Environment, University of Leeds, Leeds, UK.
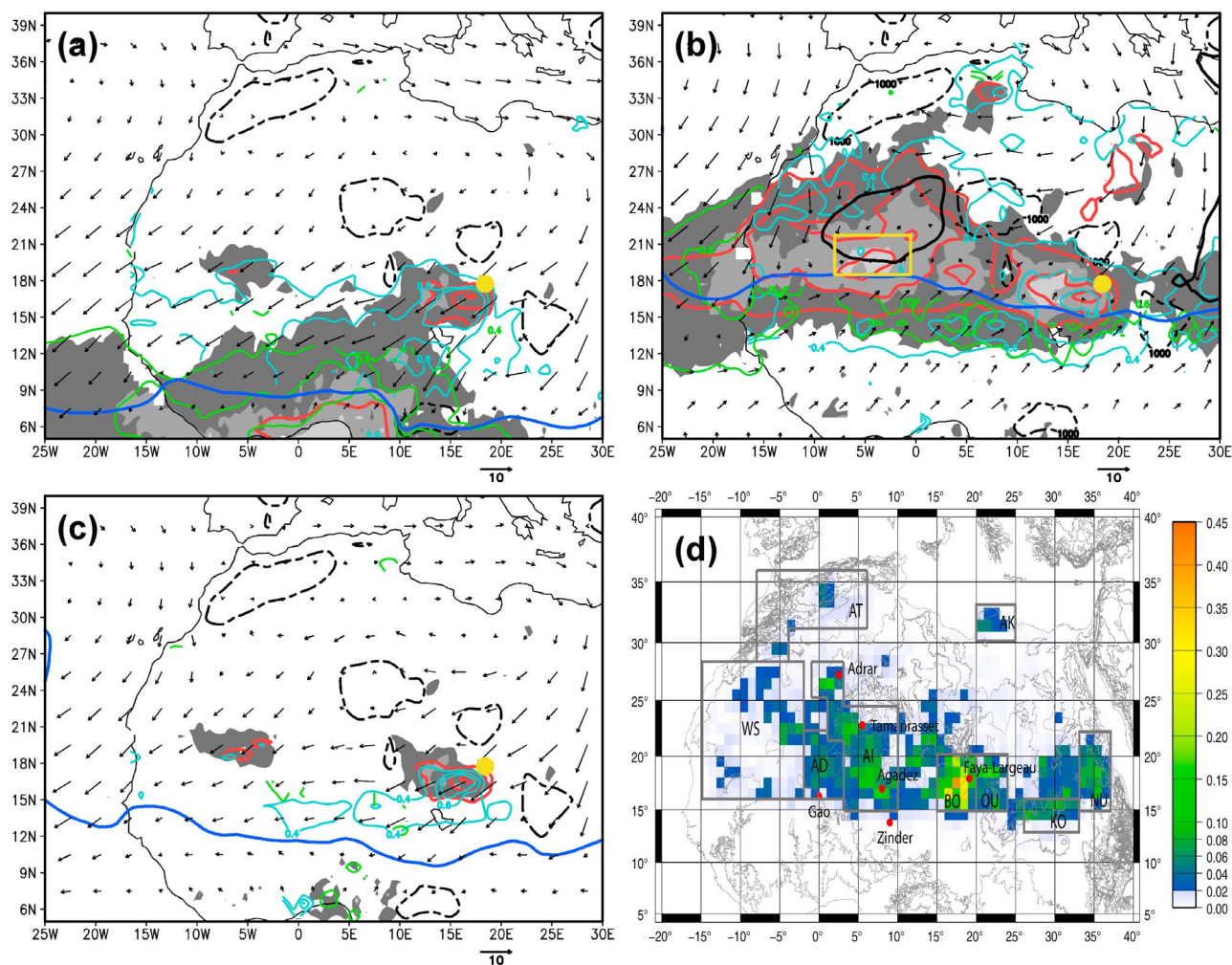[2]Department of Geography, University of Sussex, Brighton, UK.

Figure 1. Aerosols over the Sahara as estimated by satellite. (a–c) Average seasonal AOT from MISR (gray shaded), MODIS Deep Blue (cyan contour), MODIS collection 5 (green contour, over ocean and dark land surfaces south of ~15°N only), and the absorbing *AI* from TOMS (red contours). Seasons shown are the January–March (Figure 1a) and June–September dust seasons (Figure 1b) and the October–November dust-minimum season (Figure 1c). AOT shading and contour intervals are 0.4, 0.6, and 0.8; *AI* contours are 1.5, 2.0, and 2.5. To illustrate structural controls on dust distribution, the plots also show the mean 925 hPa winds (arrows), the mean position of the intertropical discontinuity (solid blue line, as defined by the 10 g kg^{-1} contour of 925 hPa specific humidity from ECMWF Re-Analysis (ERA)-Interim data), and the 1000 m surface elevation contour (dashed black contour). In Figure 1b, the mean position of the Saharan heat low core is indicated by the 1008 hPa contour of mean sea level pressure (thick black solid line). The Bodélé Depression (yellow dot) and the West African summertime dust hot spot (yellow box) are marked. Note that particularly during winter months, the AOT estimates south of ~13°N include contributions from both dust and biomass burning aerosols. (d) Mean annual dust source activation frequency as estimated from the SEVIRI dust product [*Schepanski et al.*, 2009, Figure 1].

African monsoon system [*Peyrillé et al.*, 2007; *Biasutti et al.*, 2009]. The Sahara is also a key location for tropical-extratropical interactions [*Knippertz*, 2007].

[4] Until recently, the climate of the region remained relatively poorly understood, in part because of a lack of observations. However, there have been a number of important recent developments, which have combined to advance our understanding of the emission and transport of Saharan dust. Several field studies have provided invaluable observational data, which illuminate our understanding of dust processes. These include the Bodélé Dust Experiment (BoDEx)

in 2005 [*Washington et al.*, 2006; *Todd et al.*, 2007], the African Monsoon Multidisciplinary Analysis (AMMA) in 2006 [*Redelsperger et al.*, 2006], the Dust and Biomass Experiment (DABEX) in 2006 [*Haywood et al.*, 2008], Dust Outflow and Deposition to the Ocean (DODO) in 2006 [*McConnell et al.*, 2008], the Geostationary Earth Radiation Budget Intercomparison of Longwave and Shortwave Radiation (GERBILS) in 2007 [*Haywood et al.*, 2011a], the Saharan Mineral Dust Experiment (SAMUM) in 2006 and 2008 [*Heintzenberg*, 2009; *Ansmann et al.*, 2011], and Fennec in 2011. Figure 2 gives an overview of the study
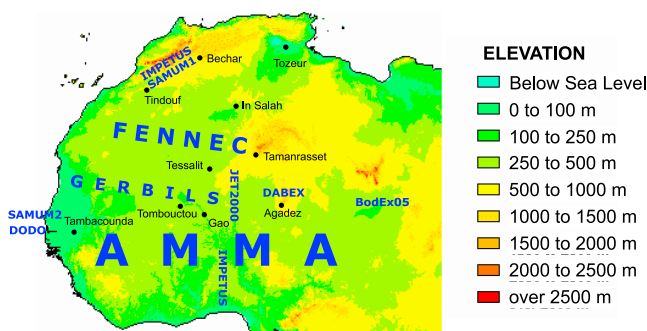
Figure 2. Study areas of recent dust field campaigns (in blue, see text for more details). The map also shows surface topography (shaded) and the locations of currently or formerly active radiosonde stations of interest for Saharan dust emission (in black). Map developed by U.S. Geological Survey EROS Data Center.

areas of these campaigns showing a bias toward the desert margins that are logistically more accessible. Only Fennec took measurements in the central Sahara, a region more than half the size of Europe. Eastern parts have received even less attention, so that the Sahara as a whole still remains a vastly undersampled region.

[5] The advent of new satellite sensors with improved observing capabilities for dust (notably the Meteosat Second Generation (MSG) Spinning Enhanced Visible and Infrared Imager (SEVIRI) [*Brindley and Ignatov*, 2006; *Thomas et al.*, 2007], Multiangle Imaging Spectroradiometer (MISR) [*Kalashnikova and Kahn*, 2008; *Kahn et al.*, 2009], and Cloud-Aerosol Lidar with Orthogonal Polarization (CALIOP) [*Winker et al.*, 2009]) as well as new algorithms for other satellite data (e.g., Moderate Resolution Imaging Spectroradiometer (MODIS) Deep Blue [*Hsu et al.*, 2004]) have combined to radically improve our ability to monitor and understand aerosol processes. At the same time, there has been a rapid development of off-line and coupled dust aerosol–atmosphere models for operational weather, air quality, and dust hazard forecasting and for Earth system research purposes.

[6] Aided by these developments there has been a substantive advance in our understanding of dust aerosols from the Sahara. This review will provide a synthesis of these developments and provide a comprehensive account of the state-of-the-art knowledge of the meteorological processes by which Saharan mineral dust aerosol is generated, distributed, and transported over the region as well as implications for representation of these in models and for weather forecast and climate prediction. This paper focuses on the most fundamental stages of the dust "cycle": the lifting of dust aerosol and the subsequent vertical and horizontal mixing and advection. It is these processes that determine the fine detail of the 3-D structure of the large-scale dust plumes over the region. This in turn strongly influences the nature of the direct, indirect, and semidirect effects on climate. Specifically, this paper considers recent advances in understanding the various multiscale meteorological phenomena that generate dust plumes, from microscale dry

convective vortices; through mesoscale circulation features including low-level jets (LLJ) and those associated with moist convection; to synoptic scale weather systems in the tropical, subtropical, and midlatitude atmosphere. These processes characteristically have a strong relationship with diurnal and seasonal cycles. The recent advances listed above are such that we now have a more complete picture of dust generation processes, although many details and their relative importance are still unclear.

[7] This paper is organized as follows: Section 2 provides the relevant background information that motivates our interest in this topic, including an overview of the role of mineral dust in the Earth system and the state of the art in monitoring and modeling the global dust budget. More detailed discussions of these aspects can be found in recent review articles by *Maher et al.* [2010] and *Shao et al.* [2011]. Section 3 then provides detail on the spatiotemporal structure of the dust plume and its meteorological drivers as well as implications for modeling. We conclude with a reflection on the state of the art and perspective on priorities for the future in Section 4.

2. THE CONTEXT

2.1. Dust in the Earth System

[8] The direct and indirect effects of aerosols constitute the largest uncertainties in our knowledge of the radiative forcing of the climate system [*Forster et al.*, 2007]. Mineral dust released from natural soils through wind erosion is estimated to contribute at least 80% to the total dust budget [*Forster et al.*, 2007] and more than half to the total global aerosol burden [*Textor et al.*, 2006]. Once airborne, dust can be mixed to great heights and can be transported over long distances. Dust in the atmosphere affects both climate and weather through the following processes:

[9] 1. Dust aerosols have a direct effect on the shortwave and longwave radiative flux through scattering and absorption. The global net top-of-the-atmosphere direct radiative forcing is on the order of -0.3 W m^{-2} with a range of -0.56 to $+0.1$ on the basis of model studies [*Forster et al.*, 2007]. There are large regional variations depending on the characteristics of the underlying surface [*Haywood et al.*, 2001, 2011b].

[10] 2. Dust aerosols have an indirect effect on the radiation budget through affecting cloud microphysical processes. Dust particles that have undergone chemical or physical processing in the atmosphere, for example, through coating with sulphates, can act as cloud condensation nuclei, affecting radiation indirectly through factors such as cloud albedo, precipitation efficiency, cloud lifetime, and cloud height [e.g., *Rosenfeld et al.*, 2001; *Kaufman et al.*, 2005; *Min et al.*, 2009; *Klüser and Holzer-Popp*, 2010]. In addition, mineral dust particles are the dominant natural ice-nucleating aerosol, leading to a faster glaciation of convective clouds [*Richardson et al.*, 2007].

[11] 3. A semidirect effect of dust is generated by absorptional heating within dust layers, which changes relative humidity and vertical stability with potential effects on

clouds, precipitation [*Solmon et al.*, 2008; *Klüser and Holzer-Popp*, 2010], and even tropical cyclone development [*Dunion and Velden*, 2004].

[12] 4. Dust provides a surface for atmospheric chemistry and can thereby mediate chemical cycles of, e.g., sulphates [*Desboeufs and Cautenet*, 2005; *Kandler et al.*, 2007] and ozone [*de Reus et al.*, 2000; *Michel et al.*, 2003].

[13] It has been shown that including effects of airborne dust into numerical models has a positive impact on weather and climate simulations [*Tompkins et al.*, 2005; *Pérez et al.*, 2006; *Chaboureau et al.*, 2007; *Rodwell and Jung*, 2008].

[14] Dust is removed from the atmosphere through gravitational sedimentation and turbulence (dry deposition) and through scavenging in precipitating clouds (wet deposition). Deposition affects climate by changing the albedo of snow and ice surfaces [*Warren and Wiscombe*, 1980; *Painter et al.*, 2007] and through biogeochemical processes in the ocean (phytoplankton) [*Erickson et al.*, 2003; *Fasham*, 2003; *Jickells et al.*, 2005] and on land [*Swap et al.*, 1992; *Okin et al.*, 2004] with important ramifications on the carbon cycle (see *Shao et al.* [2011] for a review on this topic). *Swap et al.* [1992] were the first to suggest that Saharan dust contributes to the nutrient budget of the Amazon ecosystems, which has been quantified in more recent studies [*Koren et al.*, 2006; *Ansmann et al.*, 2009a; *Ben-Ami et al.*, 2010; *Bristow et al.*, 2010]. The amount and characteristics of dust deposited in soils, glaciers, and sediments are used as indicators of climate and environmental changes on long timescales [*Lambert et al.*, 2008; *Sima et al.*, 2009; *Stuut et al.*, 2009; *Maher et al.*, 2010, and references therein; *Mulitza et al.*, 2010]. Dust has been discussed as a potential climate feedback in glacial-interglacial cycles [*Krinner et al.*, 2006; *Winckler et al.*, 2008] and for the modern climate because of interactions between dust, precipitation, and the land surface [*Rosenfeld et al.*, 2001; *Yoshioka et al.*, 2007; *Hui et al.*, 2008]. Given the complex role of dust aerosols in the Earth system, reliable quantitative estimates of the three main processes of the global dust budget, emission, transport, and deposition, are necessary for a full understanding of its role in the Earth system.

2.2. Monitoring the Dust Distribution

[15] Scientists utilize ground-based, airborne, and satellite instruments to measure various aspects of atmospheric dust including AOT, size distribution, mass concentration, vertical distribution, shape, and optical properties. Particularly because emission and deposition are rarely measured in situ and difficult to estimate from space, the current network does not provide enough observational constraints for a complete quantification of the dust budget [*Tegen and Schepanski*, 2009]. Nevertheless, advances in satellite sensors in recent years have illuminated our understanding considerably. A summary of existing satellite records of relevance with their relative strengths and weaknesses is provided in Table 1. For a more detailed review of recent developments, see *Mishchenko et al.* [2007] and *Tanré* [2010]. By their nature, satellite instruments provide indirect observations of radiances, from which parameters such

as amount, size, shape, optical properties, and elevation must be inferred. The most important products of the now extensive satellite record are (1) a near-global, long-term record of aerosol indices and AOT available from early satellite sensors such as Total Ozone Mapping Spectrometer (TOMS); (2) the ability to distinguish aerosol types in transport plumes on the basis of physical properties; and (3) more spatially and temporally resolved properties of atmospheric aerosols from the more recent sensors, including estimates directly over the Sahara desert, most notably from MODIS Deep Blue, MISR, Ozone Monitoring Instrument (OMI), CALIOP, ICESat, and SEVIRI (see Table 1 for more details). Recent developments of particular relevance to understanding Saharan dust processes are (1) the ability to retrieve quantitative AOT estimates over bright desert surfaces at high spatial resolution from nadir-viewing MODIS data (the "Deep Blue" algorithm of *Hsu et al.* [2004]) and from multiangle visible data from MISR [*Diner et al.*, 2005]; (2) estimates of AOT at 15 min temporal resolution from SEVIRI visible and infrared channels [*Brindley and Ignatov*, 2006; *Thomas et al.*, 2007; *Carboni et al.*, 2007], in addition to the qualitative SEVIRI dust product (see "Best practices for RGB compositing of multi-spectral imagery," European Organisation for the Exploitation of Meteorological Satellites guide, available at http://oiswww.eumetsat.org/SDDI/html/doc/best_practices.pdf; an example is shown in Figure 3a); (3) estimates of aerosol properties from Polarization and Anisotropy of Reflectances for Atmospheric Sciences coupled with Observations from a Lidar (PARASOL); and (4) remarkably detailed vertical profiles of aerosol backscatter from the CALIOP (and to a lesser extent ICESat) spaceborne lidar, albeit with a limited temporal sampling. The example given in Figure 3b demonstrates clear evidence of a widespread deep dust layer over the Sahara. The remainder of the paper will further illustrate how these new data sources have enabled notable advances in our understanding of aerosol emission and transport processes as well as our ability to validate model performance and highlight model limitations.

[16] It should be pointed out, however, that no single satellite instrument or retrieval is without limitations. Uncertainties have manifold causes including cloud contamination and assumptions on optical properties and perhaps most importantly by variability in surface albedo and emissivity over land. No current sensor can detect aerosols beneath thick cloud layers and thick dust is difficult to distinguish from cirrus clouds at visible wavelengths [*Roskovensky and Liou*, 2005]. All AOT products are originally designed to sample all aerosol types together and only a few studies have attempted to filter out a dust signal by making certain assumptions about optical properties [*Evan et al.*, 2006; *Ginoux et al.*, 2010; *Klüser et al.*, 2011]. The desert dust retrieval intercomparison (initial results of *Carboni et al.* [2009]) compared a sample of 15 satellite algorithms over the Sahara for a limited period during March 2006. Results show that although most algorithms correlate well with Aerosol Robotic Network (AERONET) AOT, the standard error in mean monthly AOT between the methods varied between ~0.5 and 1.0, broadly proportional to mean AOT,

TABLE 1. Summary of Satellite Sensors for Aerosol Retrievals[a]

Instrument	Spectral Characteristics	Record Length	Space/Time Resolution	AOT	Retrieval Coverage					Other Strengths/Limitations and Key References
					Desert	Other Land	Sea	Day	Night	
OMI[b]	UV channels (312–380 nm)	2004 to present	13 × 24 km; daily	Yes	Yes	Yes	Yes	Yes	No	AOT, single scattering albedo, and absorbing aerosol index; longest near continuous record (with OMI). Subpixel cloud contamination, sensitivity to aerosol layer height [Torres et al., 1998].
TOMS[b]	UV channels (312–380 nm)	1979–1993; 1996–2005	50 km; daily	Yes	Yes	Yes	Yes	Yes	No	AOT, single scattering albedo, and absorbing aerosol index; longest near continuous record (with OMI). Subpixel cloud contamination, sensitivity to aerosol layer height [Torres et al., 1998].
MODIS 5.1 standard algorithm	Visible channels (412–670 nm)	2000 to present	10 km; twice daily (daytime)	Yes	No	Yes	Yes	Yes	No	AOT and Ångström coefficient; fine mode fraction, effective radius (ocean only); asymmetry factor (ocean only); and high spatial resolution with extensive time coverage. Cloud free only [Remer et al., 2005].
MODIS Deep Blue[b]	Visible channels plus UV blue (412–670 nm)	2002 to present	10 km; twice daily	Yes	Yes	Yes	Yes	Yes	No	AOT over oceans and land and near global spatial extent at high spatial resolution and with extensive time coverage. Cloud free only [Hsu et al., 2004].
MISR[b]	Visible and near infrared channels with multiple viewing angles	2000 to present	17.6 km; 9 day global repeat cycle	Yes	Yes	Yes	Yes	Yes	No	AOT; Ångström exponent; small, medium, and large fractions; nonspherical fraction; and single scattering albedo over land and ocean with high accuracy. Cloud free only [Diner et al., 2005].
SEVIRI[b]	Visible, near, mid-, and thermal infrared channels	2002 to present	3 km nadir; 15 min	Yes	Yes	Yes	Yes	Yes	Yes (false color only)	AOT and dust false color product; high space-time resolution. Day and night for qualitative products. Cloud free only [Brindley and Ignatov, 2006; Thomas et al., 2007].
Advanced very high resolution radiometer (AVHRR)	Visible and near infrared channels	1981 to present	4 km; daily	Yes	No	No	Yes	Yes	No	AOT and Ångström coefficient; long continuous record. Cloud free only [Husar et al., 1997; Evan et al., 2006].
Advanced Along Track Scanning Radiometer (AATSR)	Visible and near infrared channels	1995 to present	3 × 4 km; 3 day repeat cycle	Yes	No	Yes	Yes	Yes	No	AOT and Ångström coefficient. High spatial resolution. Cloud free only [Thomas et al., 2009].
Medium-Resolution Imaging Spectrometer (MERIS)	Visible channels	1995 to present	~1 km; 3 day repeat cycle	Yes	No	Yes	Yes	Yes	No	AOT and Ångström coefficient. High spatial resolution. Cloud free only [Ramon and Santer, 2001].

TABLE 1. (continued)

Instrument	Spectral Characteristics	Record Length	Space/Time Resolution	AOT	Retrieval Coverage					Other Strengths/Limitations and Key References
					Desert	Other Land	Sea	Day	Night	
POLDER	Spectral, directional, and polarized visible radiances	1997 to present	20 km; daily	Yes	No[c]	No[c]	Yes	Yes	No	AOT, Ångström coefficient, fine mode, and nonspherical fractions over ocean (operational) and land (under development). Cloud free only [Herman et al., 2005; Dubovik et al., 2011].
Atmospheric Infrared Sounder (AIRS)	Infrared hyperspectral sounding channels	2003 to present	1°; twice daily (day and night)	Yes	No[c]	No[c]	Yes	Yes	Yes	AOT at 10 μm, aerosol effective radius, and mean aerosol layer height. Day and night retrievals.
Infrared Atmospheric Sounding Interferometer (IASI)	Infrared hyperspectral sounding channels	2007 to present	1°; twice daily (day and night)	Yes	No	No	Yes	Yes	Yes	AOT at 10 μm, aerosol effective radius, mean aerosol layer height. Day and night retrievals. Cloud free only.
CALIOP[b]	Polarization lidar (532 and 1064 nm)	2006 to present	30 m vertical, 300 m horizontal; 16 day repeat cycle	Yes	Yes	Yes	Yes	Yes	Yes	Vertical profile of aerosol backscatter and aerosol mask over land and ocean; cloud contamination; poor temporal sampling [Winker et al., 2009].
ICESat[b]	Laser altimeter and green channel	2003–2010 (3 months per year)	91 day repeat cycle	No	Yes	Yes	Yes	Yes	Yes	Vertical profile of aerosol over land and ocean. Cloud contamination; very low temporal sampling [Schutz et al., 2005; Spinhirne et al., 2005].

[a]All sensors provide near global coverage except SEVIRI which has a geostationary satellite view centered on 0°N, 0°E.
[b]These rows highlight those instruments which currently provide estimates directly over desert surfaces.
[c]Land retrievals under development [DeSouza-Mechado et al., 2006; Pierangelo et al., 2004; Peyridieu et al., 2010].
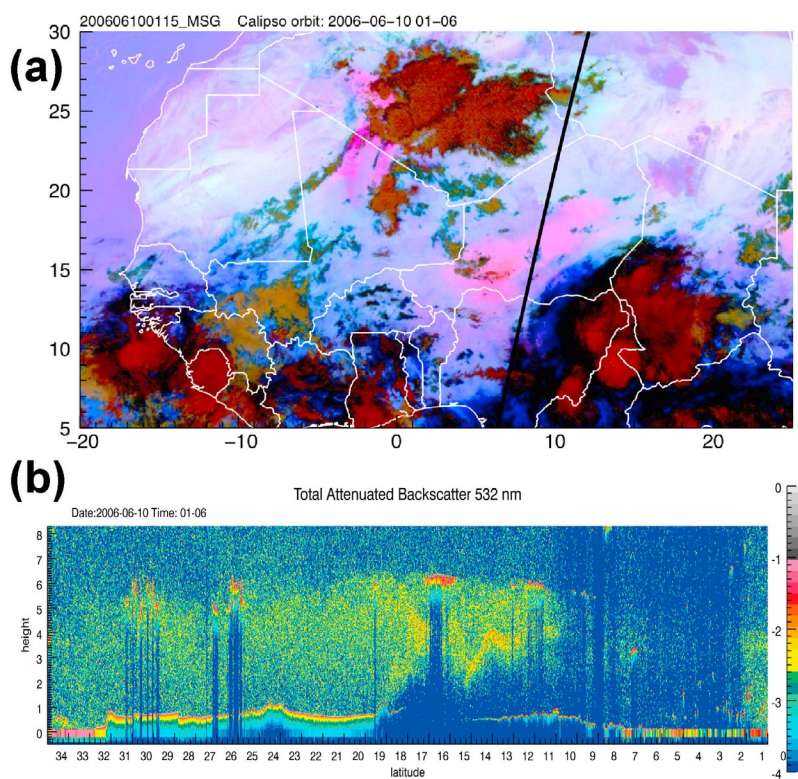
Figure 3. Example of a recent advance in Earth observation of dust aerosols. (a) MSG SEVIRI IR dust product for 0115 UTC 10 June 2006. Dust appears pink in these images and clouds appear red (deep, high), black (shallow, high), orange (midlevel), and green/blue (low). (b) The 532 nm total attenuated backscatter ($km^{-1}\ sr^{-1}$) from CALIOP with latitude marked on the x axis (horizontal track shown in black in Figure 3a, only section between Nigeria and the Libyan coast shown) around the same time. The deep dust layer over the Sahara between 20°N and 25°N and Saharan dust overriding the shallow monsoon layer over southern West Africa south of $\sim$19°N stand out in Figure 3b.

such that absolute uncertainties remain relatively high. Global scale intercomparisons indicate far greater agreement between aerosol algorithms over ocean than land [*Poulsen et al.*, 2009; *Mishchenko et al.*, 2010; *Kittaka et al.*, 2011]. There is a clear need for more extensive, quantitative intercomparison and understanding of the sources of uncertainty, especially over deserts. We can anticipate that further advances in Earth observation of aerosols will emerge from new algorithm development and integration of multiple sensors [e.g., *Christopher et al.*, 2011].

[17] While satellites provide unparalleled spatial and temporal coverage, surface-based sensors play an important role too (not least as validation for satellite products). The global AERONET network of almost 500 surface-based Sun photometers [*Holben et al.*, 1998] provides high-quality retrievals of AOT and of aerosol optical and physical properties. However, coverage in the Sahara is particularly sparse. The recent field campaigns over North Africa listed in section 1 (see Figure 2) have involved the deployment of sophisticated surface-based instrumentation to directly measure aerosol and related meteorological properties with high precision. These include standard meteorological instruments, aerosol lidar, optical particle counters, and various dust samplers to measure emission and deposition as well as detailed optical and physical properties of aerosols (see Figures 5a and 14b for examples). In many cases (AMMA, DABEX, SAMUM, and Fennec), these surface observations are complemented with similar measurements from airborne instruments on research aircraft, providing very detailed information on processes in horizontal and vertical directions. All, however, are limited by relatively short observation periods over limited domains.

2.3. Issues in Modeling Dust Processes

[18] Recent years have seen a veritable boom in the development and implementation of dust modules in weather and climate models for a large range of applications reaching from modeling systems for regional or global air quality and dust forecasting (e.g., Global and Regional Earth-System Monitoring Using Satellite and In Situ Data (GEMS) [*Hollingsworth et al.*, 2008], Monitoring Atmospheric Composition and Climate (MACC) [*Morcrette et al.*, 2008], Dust Regional Atmospheric Model (DREAM) [*Nickovic et al.*, 2001], and Integrated Community Limited Area Modeling System (ICLAMS) [*Solomos et al.*, 2011]), through global off-line aerosol-chemistry transport models used for process
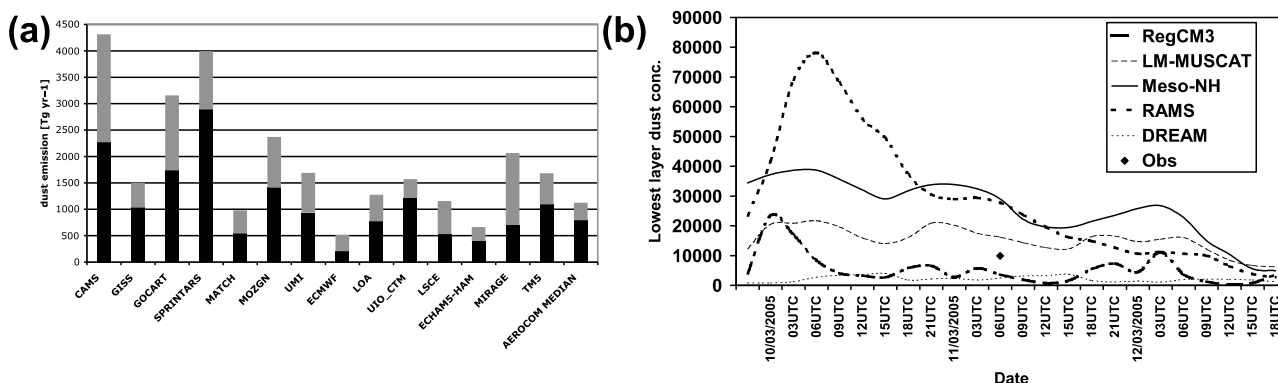
Figure 4. Uncertainty in model estimates of dust emission at the global and local scales. (a) AeroCom model intercomparison of annual global (gray bars) and North African (black bars) dust emission based on data from *Huneeus et al.* [2011]. (b) Time series of model simulated dust concentration in lowest layer (μg m^{-3}) at the location of Chicha, Chad, during the BoDEx field campaign in March 2005 showing marked model disagreement and temporal trends [*Todd et al.*, 2008a, Figure 8]. Only one observation is available for this period (marked as a black diamond).

studies (e.g., Global Model of Aerosol Processes (GLOMAP) [*Spracklen et al.*, 2005] and CHIMERE-DUST [*Menut et al.*, 2009]), to fully coupled Earth system models employed for climate projections (e.g., Quantifying and Understanding the

Earth System (QUEST) Earth System Model (QESM; http://www.quest-esm.ac.uk/) and Community Climate System Model (CCSM) [*Mahowald et al.*, 2011]). It is notable that the World Meteorological Organization (WMO) recently
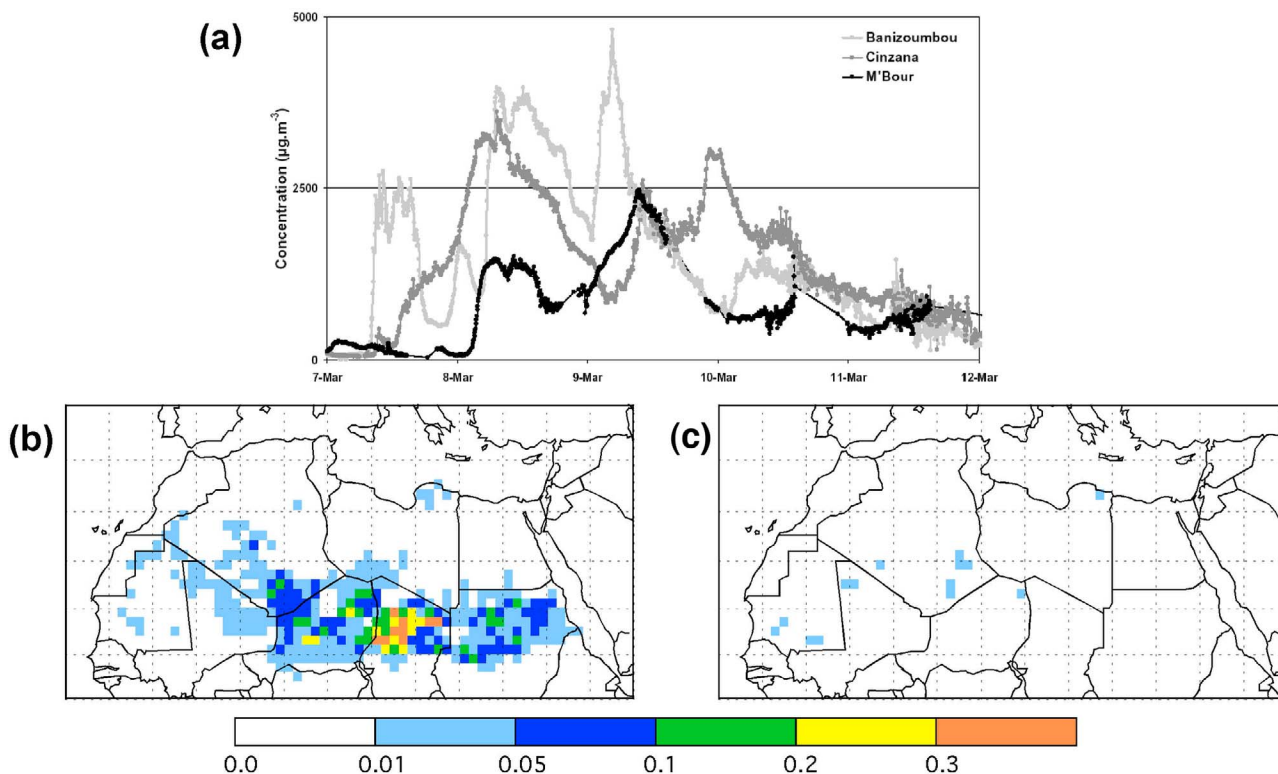

Figure 5. Diurnal cycle of dust emission. (a) The 5 min mean PM$_{10}$ concentrations measured along the AMMA Sahelian dust transect at Banizoumbou (Niger), Cinzana (Mali), and M'Bour (Senegal) from 7 to 12 March 2006 [*Marticorena et al.*, 2010, Figure 10]. The time evolution shows rapid changes in surface concentrations due to changes in local wind speed and advection from sources upstream. Frequencies of dust source activation as identified from the infrared channels of SEVIRI during boreal winter (December–February) for (b) 0300–0900 and (c) 1200–0000 UTC [from *Schepanski et al.*, 2009, Figure 2]. The shorter morning period shows substantially more emission events across large parts of the southern Sahara.

established the Sand and Dust Storm Warning Advisory and Assessment System (SDS-WAS; http://www.wmo.int/pages/prog/arep/wwrp/new/Sand_and_Dust_Storm.html) to enhance the ability of countries to deliver timely and quality sand and dust storm forecasts, observations, information, and knowledge to users. Within this program, the Northern Africa-Middle East-Europe Regional Center aims to lead the development and implementation of a system for dust observation and forecast and currently distributes forecasts over North Africa from eight modeling centers.

[19] In the framework of the Global Aerosol Model Intercomparison (AeroCom) initiative [*Schulz et al.*, 2009], the dust budget in 15 global models driven by prescribed or nudged analyzed meteorological fields were compared [*Textor et al.*, 2006; *Huneeus et al.*, 2011]. All diagnostic parameters characterizing the dust budget show a large spread with estimates for both global and North African dust emissions differing by a factor of about 5 (Figure 4a). These uncertainties are attributed to differences in (1) dust emission parameterization [*Zender et al.*, 2004]; (2) soil properties, including soil moisture; and (3) representation of peak winds. Because of the high sensitivity of dust flux to the high tail of the wind speed distribution, the usage of different meteorological "driver" fields (e.g., European Centre for Medium-Range Weather Forecasts (ECMWF) versus National Centers for Environmental Prediction reanalysis) alone can produce larger differences than different dust emission schemes [*Luo et al.*, 2003; *Menut*, 2008]. Using wind fields generated by free running regional or global models, as necessary for air quality forecasts or climate projections, further enhances the wind-related uncertainties [*Timmreck and Schulz*, 2004]. A regional dust model intercomparison for the Bodélé Depression during BoDEx by *Todd et al.* [2008a] shows differences in emission and loading of around 1 order of magnitude (Figure 4b). Major obstacles to reducing these uncertainties are the lack of available dust emission measurements to validate emission parameterizations near source areas (see section 2.2 for more details).

[20] Uncertainties in emissions have impacts on the entire dust budget. Because of a stronger observational constraint on dust burden through satellite AOT retrievals, models are often "tuned" with respect to this parameter (see section 2.3.1 for more details), resulting in a diversity among the AeroCom models of 40%, which is smaller than that for emission and deposition [*Textor et al.*, 2006]. Prescribing emissions has a surprisingly small effect on dust burden [*Textor et al.*, 2007, Table 2], suggesting that tuning creates compensational effects between emission and deposition. It is, therefore, believed that source strength is one of the major limiting factors in simulating aerosol fields [*Textor et al.*, 2006]. Any improvement in the representation of dust emission in models will therefore improve estimates of both dust loading and deposition, calling for a better understanding of the involved mechanisms at the process level [*Textor et al.*, 2007]. This in turn is crucial for radiative forcing and cloud effects (loading) and biogeochemical and surface albedo effects (deposition).

2.3.1. Dust Emission Parameterization

[21] Dust emission involves complex, nonlinear processes governed by meteorology and the state and properties of land surfaces. Direct in situ field measurement typically observe emission over a few tens of square meters at most [e.g., *Houser and Nickling*, 2001], so that measurement at the scale of most atmospheric models are rather difficult. The currently ongoing project DO4 Models: Dust Observation (http://www.geog.ox.ac.uk/research/climate/projects/do4models.html) aims to observe emission at a coarse, model-relevant scale at a field site in Botswana. To date, much of what is known about these processes has been obtained from microscale (local) experiments in the field and wind tunnels and theoretical studies [e.g., *Marticorena and Bergametti*, 1995; *Alfaro et al.*, 1998; *Shao and Mikami*, 2005; *Ishizuka et al.*, 2008; *Okin*, 2008; *Li et al.*, 2010; *Kok*, 2011]. The early work of *Bagnold* [1935, 1937] suggested that dust particles are released to the atmosphere through three mechanisms: (1) the direct aerodynamic entrainment or suspension of particles, (2) saltation bombardment, and (3) aggregate disintegration. Emission schemes parameterize some or all of these processes and are classified as more or less physically based, depending on the number of processes explicitly represented. Dust emission models are too numerous to describe here individually, but, in general, global models tend to incorporate simple schemes and regional models utilize more physically based schemes (see short summary in chapter 6.1 of *Shao et al.* [2011]).

[22] Simple schemes parameterize the vertical flux of emitted mineral aerosols into the atmosphere as a function of the third (or fourth) power of the difference between the surface wind speed u and a fixed threshold u_t for $u > u_t$. Other schemes use the friction velocity, u_*, instead. Here u_* is the square root of the kinematic stress at the surface and is usually calculated from wind at 10 m and surface roughness. In contrast, more physically based schemes [*Marticorena and Bergametti*, 1995; *Shao et al.*, 1996] explicitly calculate (1) the size-resolved horizontal flux (saltation) as a function of friction velocity above the threshold, which depends on the surface characteristics of soil grain size distribution, crusting, moisture content, snow, and vegetation cover and then (2) the resulting vertical dust fluxes from soil aggregate bombardment and disintegration, either as a function of particle kinetic energy [*Shao et al.*, 1996; *Alfaro and Gomes*, 2001] or through a volume removal relationship [*Lu and Shao*, 1999; *Shao*, 2004]. Many schemes include a scaling parameter to represent source "intensity" to tune emissions. For example, preferential sources have been identified by colocation of peak TOMS aerosol index (*AI*) and topographic lows [*Ginoux et al.*, 2001; *Prospero et al.*, 2002]. Others use more physical parameters such as the grid cell erodible fraction, i.e., the part of the surface which is not protected from wind erosion by roughness elements [e.g., *Laurent et al.*, 2006]. Generally speaking there is a substantial disagreement between different methods to identify sources [see *Formenti et al.*, 2011, Figure 1].

[23] Dust emission schemes require both meteorological and land surface characteristics at the temporal and spatial scales pertinent to dust emission processes such as high-resolution surface stresses, particle size distribution, binding energies, etc. Such information is hardly ever available, even for the highest-resolution regional models (a few kilometers grid spacing). As a result, because of remaining large uncertainties associated with representing the very hetero-geneous soil and land surface physical characteristics and wind regimes, many modelers have introduced explicit or implicit tuning parameters into the schemes, which enables emission to be calibrated such that the resulting dust burden in the atmosphere is consistent with measured AOTs from surface or satellite [*Cakmur et al.*, 2006]. Even in applying the most physically based schemes many parameters, espe-cially soil characteristics, are not sufficiently well con-strained, so empirically derived constants are commonly used in process equations. Examples include the constants in the soil moisture correction and in the derivation of vertical dust flux from horizontal saltation flux (the "sandblasting efficiency") [*Marticorena and Bergametti*, 1995; *Alfaro and Gomes*, 2001; *Shao*, 2004]. It is highly likely that these constants are in effect scale and location dependent and that varying these could be used to tune emission.

[24] Not surprisingly, model intercomparison projects typically indicate high uncertainty in dust emission estimates [e.g., *Textor et al.*, 2006; *Todd et al.*, 2008a; *Huneeus et al.*, 2011], but identifying and ranking the specific sources of model error is difficult. To address this, a number of recent studies have sought to systematically quantify the uncer-tainty associated with each stage in various physically based dust schemes. *Darmenova et al.* [2009] noted from the sensitivity experiments of the *Marticorena and Bergametti* [1995] and *Shao et al.* [1996] schemes that horizontal dust flux is most sensitive to friction velocity, with land surface parameters important only for lower wind speed events, highlighting the priority need to reduce uncertainty in meteorological fields. Nevertheless, sensitivity experiments using identical meteorology show that differences in monthly emission over the main Asian dust source regions can greatly exceed a factor of 2 as a result of the combined differences between two schemes. *Kang et al.* [2011] explicitly analyzed the sensitivity to three different vertical flux parameterizations for a 5 day Asian dust event. Total emission estimates vary by more than a factor of 6. Note that differences in scale and location between these two studies make direct quantitative comparison difficult. It is clear, however, that uncertainty associated with parameterization of the dust emission processes remains very high, resulting from incomplete physics coupled with a lack of critical land surface information.

[25] Whatever dust scheme is used, a key requirement is an accurate representation of the high tail of the u_* distri-bution. Despite the high sensitivity of emissions to near-surface peak winds [*Uno et al.*, 2006] and the comparatively large amount of available measurements of this parameter in source regions, surprisingly few studies have addressed the problem of improving the representation of u_*, which is

often simply considered as an external driving parameter. Atmospheric models used for dust simulations are mostly based on numerical weather prediction or climate models, which have not been optimized for the complex and highly energetic desert PBL. It has been suggested that coarse-resolution models cannot sufficiently represent many mete-orological processes crucial for peak wind generation and that a parameterization of subgrid wind variance is desir-able [e.g., *Cakmur et al.*, 2004]. First attempts to tackle this problem in a physical way by computing probability density functions for wind speed using turbulent kinetic energy (TKE) estimates from the model's PBL scheme report sig-nificant improvements [*Cakmur et al.*, 2004; *Grini et al.*, 2005], consistent with higher correlations of dust loadings with gustiness than with mean wind [*Engelstaedter and Washington*, 2007].

2.3.2. Deposition

[26] Dust deposition occurs through both dry deposition and wet deposition associated with cloud and precipitation processes. As such, deposition involves a complex set of physical processes for which understanding requires detailed knowledge of dust size distribution, density, particle shape, hygroscopicity, and cloud and precipitation microphysics. As it is not a focus of this review, only a very short summary is given here for completeness. Overall, the uncertainty in deposition processes and rates are at least as great as those for emission processes but have received far less attention in the literature, and there has been limited systematic evalua-tion in dust models [*Huneeus et al.*, 2011]. Estimates of total deposition based on global aerosol models range from about 700 to over 4000 Tg yr^{-1}, with wet deposition contributing from over 60% to well under 20% [*Huneeus et al.*, 2011, Table 3]. Measurements of dust deposition are conducted with traps over land and ocean but are generally few and incomplete, particularly for dry deposition. *McTainsh* [1999], for example, measured deposition rates of about 200 g m^{-2} yr^{-1} in Niger. Observations established during AMMA [*Rajot et al.*, 2008] and the International Global Atmospheric Chemistry - Deposition of Biogeochemically Important Trace Species Africa (IDAF) network (http://idaf. sedoo.fr/spip.php?rubrique3) have improved our knowledge over Sahelian and tropical West Africa. There is a large interest in the magnitude of dust input into the world's oceans because of biogeochemical implications, but current estimates disagree by a considerable amount [see *Shao et al.*, 2011, Table 2]. Because of the great source strength of the Sahara and predominant easterly flow at low levels, the North Atlantic is one of the regions with the largest dust input (on the order of 180–260 Tg yr^{-1}).

3. METEOROLOGICAL CONTROLS ON DUST DISTRIBUTION

[27] In this section, we summarize the key characteristics of the dust distribution over the Sahara (section 3.1) and review the recent research, which has sought to provide a physical explanation of these structures (section 3.2).

3.1. Spatiotemporal Structure of Saharan Dust

[28] Despite the growth of integrated surface-based observational networks such as AERONET, there remains precious few direct in situ observation of the dust budget from the Sahara. However, advances in satellite systems (see section 2.2) have facilitated new insights into the characteristic patterns of Saharan dust emission and transport and the associated effects on climate. Here we describe some of the key features of the mean horizontal and vertical dust distributions as well as their seasonal and diurnal cycles.

3.1.1. Mean Dust Distribution and Associated Seasonal Cycle

[29] Annual mean dust burden derived from all the long-term satellite data sets currently available (TOMS, OMI, MISR, and MODIS Deep Blue; see Table 1 and section 2.2 for details) show similar spatial patterns with peaks ("hot spots") immediately downwind of the Bodélé Depression in Chad and a larger area over the western Sahara (WS) with a large downwind transport plume extending from the continent over the subtropical east Atlantic (Figure 1). *Ben-Ami et al.* [2011] have recently described the mean seasonal pattern of emission and transport over the subtropical North Atlantic as an annual "triplet" of two strong dust seasons and one season with low dust loadings. The first dust season extending from November to March (Figure 1a) involves episodic dust emission events, notably from the Bodélé Depression, and dust transport within a more southern latitude and over West Africa and the Atlantic at ∼5°N, where the dust often mixes with biomass burning aerosol [e.g., *Knippertz et al.*, 2011]. The second dust season during May–September (Figure 1b) has more uniform emission frequency with strong contributions from the Bodélé Depression and WS. At this time of year, the broad WS dust hot spot is colocated with the SHL (Figure 1b). Smaller areas of high dust loadings are located along the southern foothills of the Atlas Mountains and in Libya and Egypt. The westward dust transport plume advances northward to reach about 20°N. The third season of October–December experiences low dust loadings (Figure 1c). Differences in the satellite products shown in Figure 1 are nicely illustrated by the different size of the Bodélé Plume during this season, illustrating the uncertainties discussed in section 2.2.

[30] Regarding the location of continental dust sources, work in the last decade sought to interpret the patterns of dust burden in terms of local source regions [*Prospero et al.*, 2002; *Washington et al.*, 2003; *Engelstaedter and Washington*, 2007]. This is relatively unproblematic in the case of the Bodélé Depression, where the extraordinary frequency of emission during winter from localized lacustrine deposits combined with a dominant southwestward transport ensures that the hot spot in satellite fields directly represents the activity of this singular source. Recent work on the Bodélé Depression has provided a comprehensive climatological and geomorphological explanation for its dominance as a dust source [*Washington et al.*, 2006; *Koren et al.*, 2006; *Todd et al.*, 2007]. Of course, other sources are active in winter too (notably those in the great event of

March 2006 [*Slingo et al.*, 2006; *Cavazos et al.*, 2009]), but their frequency of emission is so much lower than that of the Bodélé Depression that their emission does not emerge strongly in mean aerosol burden fields (Figure 1a).

[31] Explaining the existence of the WS hot spot is more difficult and has been a source of lively debate in the literature for a number of reasons: (1) the high dust burden is dispersed over a wider area (Figure 1b), (2) there is no single major source region with a well-understood geomorphological history [*Prospero et al.*, 2002; *Washington et al.*, 2003], (3) the few available surface station observations are not fully consistent with the strong increase in summer that some satellite products show [*Klose et al.*, 2010], and (4) the dust "season" occurs during the West African summer monsoon when the atmospheric circulation in the region leads to multiple meteorological emission mechanisms and trajectories of dispersion [*Knippertz and Todd*, 2010] (see also section 3.2). High-temporal-resolution imagery from the MSG SEVIRI has enabled more precise identification of sources through a qualitative backtracking of specific dust plumes to their sources of origin [*Schepanski et al.*, 2007]. The resulting maps of dust source activation frequency (DSAF; irrespective of magnitude, Figures 1d, 5b, and 5c) confirm the importance of the Bodélé Depression and broadly the WS but illustrate the importance of the margins of topographic features, notably the Hoggar and Aïr Mountains for the latter region. The disparity over WS between DSAF and the satellite-derived mean aerosol burden is consistent with the explanation of *Knippertz and Todd* [2010], which suggests that multiple, multiscale emission mechanisms associated with the climatological distribution of synoptic and mesoscale processes activate the various dust sources identified in the DSAF and drive the subsequent vertical and horizontal transport processes over the WS and West African sector, with the resulting distribution exhibited in Figure 1b. In the following, we will examine the meteorological processes of emission and transport that in effect drive this complex seasonal pattern in more detail.

3.1.2. Diurnal Cycle

[32] Early studies on the diurnal cycle of dustiness used synoptic station observations of horizontal visibility as an indicator and found an increase during the daytime hours with some variations between the Sahel and Sahara [*N'Tchayi Mbourou et al.*, 1997]. High-resolution surface concentrations from the AMMA Sahelian dust transect show remarkably complex diurnal changes with abrupt increases but generally confirm the daytime maximum (Figure 5a). Until recently, satellite aerosol products were limited to a fixed daily observation time by either characteristics of the satellite platform (polar-orbiting satellites in the case or TOMS, OMI, MISR, and MODIS) or the algorithm (the Infrared Difference Dust Index) [*Legrand et al.*, 1994]. As such our perspective on dust was strongly biased toward the near-noon time period. Analysis of the twice daily time series of MODIS data revealed a strong diurnal pulsing of emission from the Bodélé Depression during winter, indicating discrete "packets" of emission during daytime hours [*Koren and Kaufman*, 2004]. Subsequent analysis of the
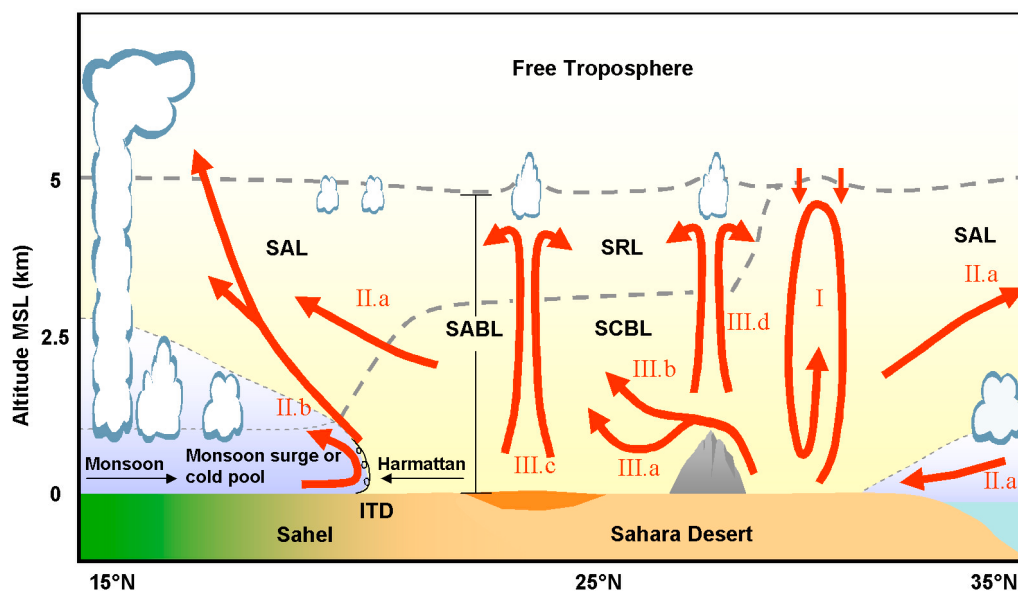
Figure 6. Schematic of the mechanisms which control the structure of the Saharan PBL and dust vertical redistribution [*Cuesta et al.*, 2009, Figure 1]. Shading (yellow or light blue) indicates air mass origin and temperature. Abbreviations stand for intertropical discontinuity (ITD), Saharan air layer (SAL), Saharan atmospheric boundary layer (SABL), Saharan convective boundary layer (SCBL), and Saharan residual layer (SRL). The numerical labels in the figure refer to sections of *Cuesta et al.* [2009]; the associated processes are described here in section 3.2.4.

number of plume trajectories across the entire Sahara from the novel 15 min SEVIRI imagery [*Schepanski et al.*, 2007, 2009] revealed the dominance of the midmorning period for dust plume initiation in all source regions in all seasons (Figures 5b and 5c show boreal winter as an example).

3.1.3. Vertical Distribution

[33] Most passive satellite and ground-based instruments can only provide column-integrated information on dust loading such as AOT (see section 2.2). Most of our knowledge on the vertical structure of dust plumes results from aircraft, surface-based, and satellite-borne aerosol lidars. While the former two are usually restricted to field campaigns or locations relatively far away from Saharan dust sources, spaceborne CALIOP now provides north-south cross sections through Saharan dust plumes in cloud-free regions (e.g., Figure 3b). Although the temporal resolution of CALIOP is poor, the widespread distribution and relatively slow dust transport allows a robust picture to emerge. These measurements have added substantial detail to our knowledge of the characteristic vertical patterns in the dust distribution, first investigated through aircraft measurements in the 1970s, particular over the continent. During winter, dust plumes remain close to the surface during transport from sources across the Sahara [*Chiapello et al.*, 1995; *Johnson et al.*, 2008; *Peyridieu et al.*, 2010; *Knippertz et al.*, 2011], with high concentrations at stations in the Sahel [*Klose et al.*, 2010; *Marticorena et al.*, 2010]. South of 10°N there is evidence of dust aerosol (often mixed with biomass burning aerosol) above 1.5 km, probably associated with vertical transport around cumulus congestus cloud systems over southern West Africa [*Knippertz et al.*, 2011].

[34] During the boreal summer, the PBL and therefore the dust layer over the Sahara and the adjacent Atlantic Ocean is substantially deeper and frequently reaches altitudes of up to 6 km above sea level [*Gamo*, 1996; *Léon et al.*, 2009; *Tesche et al.*, 2009; *Cavalieri et al.*, 2010; *Peyridieu et al.*, 2010]. This deep, hot, and dusty air mass has been termed the Saharan air layer (SAL) by *Carlson and Prospero* [1972]. Toward the fringes of the Sahara the SAL usually glides up onto the cooler low-level air masses of the southwesterly monsoon flow to the south and the maritime air of the subtropical Atlantic and Mediterranean Sea to the west and north, leading to an elevated dust layer [*Prospero and Carlson*, 1972; *Karyampudi and Carlson*, 1988]. For the continent, this behavior is nicely summarized in a schematic by *Cuesta et al.* [2009], reproduced as Figure 6 here. The example aerosol profile from CALIOP shown in Figure 3b clearly shows (1) dusty air that appears well mixed throughout the PBL ("SCBL" in Figure 6) over the Sahara, thereby extending from the distinct "cap" at about 6 km height all the way to the ground and (2) how this dust air layer overrides the low-level monsoonal southwesterlies to the south of about 18°N. Observations of surface concentrations in the Sahel show relatively low values in summer [e.g., *Marticorena et al.*, 2010, Figure 4] despite considerable AOTs, confirming the upgliding of dusty air over the monsoon layer.

3.2. Meteorological Conditions for Dust Emission and Vertical Mixing

[35] Analysis of dust and driving meteorological fields from a combination of observations from satellite and field campaigns with model simulations has advanced our

understanding of the role of the multiscale meteorological processes involved in dust emission and transport. This new knowledge provides at least qualitative explanations for the observed spatiotemporal characteristics of the Saharan dust distribution described in section 3.1. To summarize these findings, we will structure this section according to the scale of the meteorological processes from synoptic (section 3.2.2), through mesoscale (section 3.2.3), to microscale aspects (section 3.2.4). In addition, section 3.2.1 will discuss the diurnal cycle of the PBL over the Sahara and how it influences wind speed near the surface, focusing on the role of LLJs. Section 3.2.5 will conclude with some remarks on vertical and horizontal transports. Each of these sections will also discuss implications for modeling the respective process.

3.2.1. Low-Level Jets

[36] Recent studies have indicated that LLJs play a key role in Saharan dust emission and transport. The peak morning emission from the single greatest dust source of the Bodélé Depression [*Washington et al.*, 2006] and more widely across the Sahara [*Schepanski et al.*, 2009] (Figures 5b and 5c) is now known to be phase locked to the LLJ diurnal cycle. The mechanism of LLJ formation, which is found in all subtropical desert regions and which governs the (out of phase) diurnal cycles of LLJ and surface winds (and hence dust emission), is described as follows. In the free troposphere, wind speed and direction for a given location is mainly controlled by the ambient pressure gradient, leading to flow close to geostrophic balance away from the equator. Closer to the surface, turbulence and frictional effects create substantial deviations from geostrophy depending on factors such as surface roughness, wind shear, and vertical stability. Particularly, the last factor can create substantial systematic differences between day and night within the PBL and surface layer. Cloud-free and dry conditions in desert regions cause most of the high insolation during the day to be converted into sensible heating at the surface, leading to a hot, often rather deep, dry convective PBL.

[37] During the night, strong radiative cooling stabilizes the very lowest layers and effectively decouples most of the air that used to be within the PBL during the day from surface friction [*Todd et al.*, 2008b]. In areas of sufficient background pressure gradient, this decoupling leads to an inertial oscillation around the equilibrium wind (usually well approximated by the geostrophic wind) [*Blackadar*, 1957; *Van de Wiel et al.*, 2010] as schematically depicted in Figure 7a. The amplitude of the oscillation depends on the magnitude of the ageostrophic component at the time of decoupling (*D* in Figure 7a) and therefore on the background pressure gradient, latitude, and roughness of the underlying surface. Rough surfaces exert a strong frictional force and therefore a high-amplitude inertial oscillation. The oscillation period is given by 2π divided by the Coriolis parameter, *f*. For 23°N, a typical latitude in the Sahara, the oscillation period is 30.7 h. Assuming a decoupled period of 10–12 h, only about 1/3 of the oscillation can be completed, leading to highly supergeostrophic LLJ peaking before sunrise

(as shown from model experiments over the Bodélé Depression in Figure 7b).

[38] The importance of the LLJ to dust results from its relationship with surface winds. After sunrise, surface heating causes the PBL to grow in depth and mixes momentum from the jet level down to the surface. This creates the distinctive diurnal cycle with peak surface winds and dust emissions from morning to midday (Figures 5a, 7c, and 8) and the resulting erosion of the LLJ above and hence the out of phase diurnal cycle of LLJ and surface winds (Figure 7c) [*Knippertz*, 2008; *Todd et al.*, 2008b]. There are very few radiosonde observations of LLJs in the Sahara (Figure 2), but analysis data suggest a frequent occurrence throughout the year (Figure 7d shows January as an example). It should be noted here that the degree of decoupling critically depends on factors suppressing turbulence near the surface during the night. On one hand, clouds or high-column water vapor weaken the radiative cooling and therefore keep stability relatively low, leading to generally less decoupling in summer. This can lead to one or several breakdowns of the jet during the night, when the vertical shear underneath the jet core has reached a critical level, creating so-called intermittent mixing events [*Banta et al.*, 2003]. On the other hand, in situations of very strong background pressure gradients, stability might never become high enough to suppress the mechanically induced turbulence near the surface and therefore impedes a complete decoupling (see, for example, Figure 8a showing surface winds during the main dust storm days during BoDEx and Figure 5a showing a dust emission case over the Sahel).

[39] The close spatial similarity in the frequency of LLJs (Figure 7d) and dust source activation (Figures 5b and 5c) provides compelling evidence of the often dominant role of LLJs in emission, most notable in winter. Accurate model representation of the LLJ processes is therefore crucial. While state-of-the-art numerical models usually reproduce the large-scale pressure gradients that drive LLJs satisfactorily, they often struggle to reproduce the distinct diurnal cycle in near-surface winds (Figure 8a). Several studies have shown problems with temperature inversions over arid areas being too weak, leading to an underestimation of stability in the lowest layers, too little decoupling, and therefore too much vertical dispersion during the night resulting in large wind forecast errors and even phase errors [*Hanna and Yang*, 2001; *Zhong and Fast*, 2003]. These results are sensitive to vertical resolution, PBL scheme, and roughness length [*Zhang and Zheng*, 2004; *Todd et al.*, 2008b] (Figure 8b), suggesting that there is an opportunity to optimize forecast models for the Saharan sector. The work of *Todd et al.* [2008b] notwithstanding, a systematic investigation of the representation of LLJs in dust models and potential implications for emission and transport strength and diurnal cycle remains lacking.

3.2.2. Synoptic Scale

[40] It has long been known that the episodic nature of large dust events is primarily controlled by synoptic scale meteorological features [e.g., *Dubief*, 1979; *Washington and Todd*, 2005; *Schepanski and Knippertz*, 2011], but more
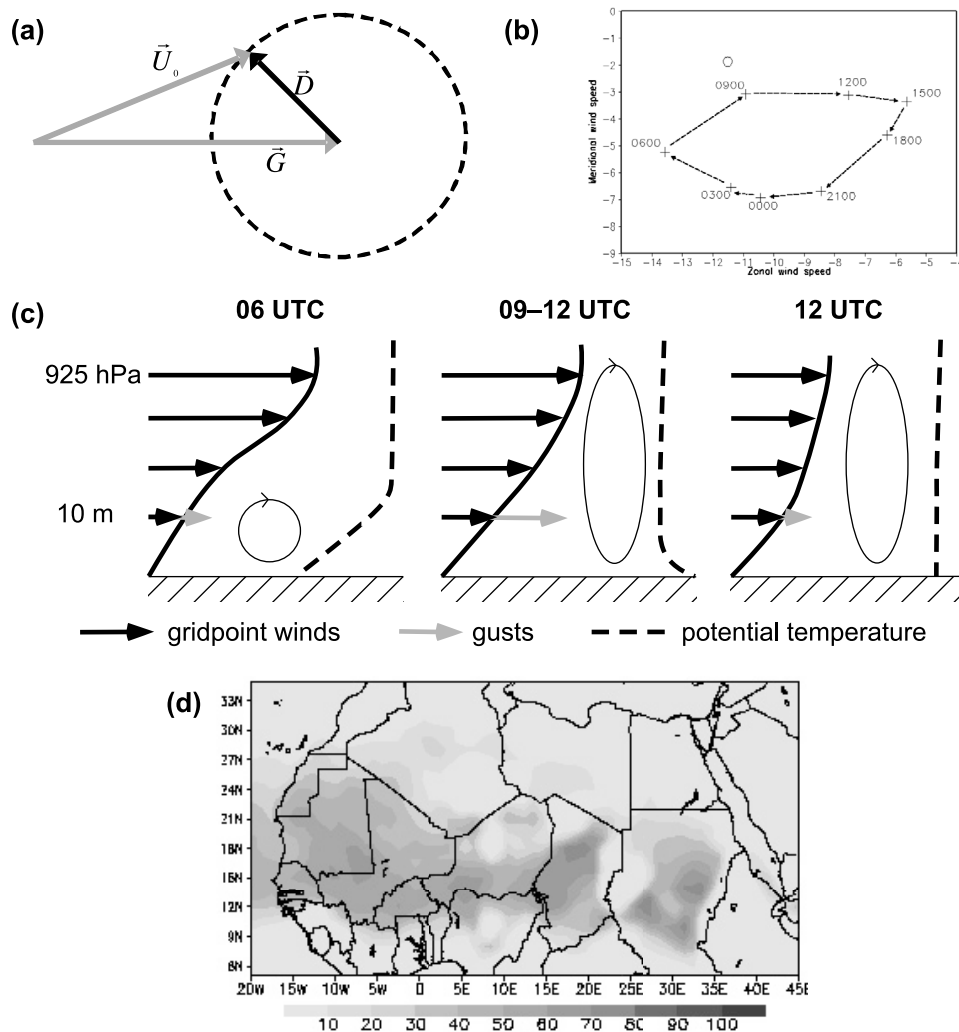
Figure 7. The LLJ and its role for dust emission. (a) Schematic showing a low-level wind vector in the evening (U_0) together with the geostrophic (G) and ageostrophic (D) wind components [*Van de Wiel et al.*, 2010, Figure 1]. The decoupling from surface friction during the night causes a clockwise (in the Northern Hemisphere) inertial oscillation of the wind vector following the dashed circle with a period of $2\pi/f$. (b) Mean diurnal cycle of winds at 940 hPa from numerical simulations over the Bodélé Depression during BoDEx in February and March 2005 providing clear evidence of an inertial oscillation [*Todd et al.*, 2008b, Figure 9a]. (c) Schematic depiction of typical changes in the vertical profile of low-level wind, gusts, potential temperature, and turbulence over the Sahara during morning hours [*Knippertz*, 2008, Figure 1] (http://www.schweizerbart.de/). The key for dust emission is the downward mixing of momentum from the nocturnal LLJ during the morning buildup of the PBL. (d) Frequency of LLJ events during January for ERA-Interim reanalysis data showing widespread occurrence through large parts of the Sahara [*Schepanski et al.*, 2009, Figure 4]. Note similarity of LLJ frequency and dust storm activation frequency in Figure 5. Figures 7a and 7b are © American Meteorological Society. Reprinted with permission.

recent analysis of the space-time distribution of dust AOT has added considerable detail to our understanding. The most important prerequisite for dust storms on this scale is the establishment of a sufficiently large surface pressure gradient to drive strong winds capable of dust emission and long-range transport. From many analyses of case study events and statistical analysis of long-term records, we now have more evidence to identify the dominant synoptic types by season.

[41] During the cool season from November to April, two patterns appear especially important. First, upper level troughs over northern Africa can trigger intense Saharan cyclones along the northern margin of the Sahara [*Alpert and Ziv*, 1989; *Bou Karam et al.*, 2010]. These systems are often related to lee cyclogenesis to the south of the Atlas Mountains and then track eastward along the Mediterranean coast (Figure 9a). They are often referred to as Khamsin cyclones in Libya and Egypt and Sharav cyclones in Middle East. Many tracks turn northward into Turkey, but some systems continue moving eastward. Incorporating moisture from the Mediterranean Sea can lead to a rapid intensification of the system and cause significant rainfall.
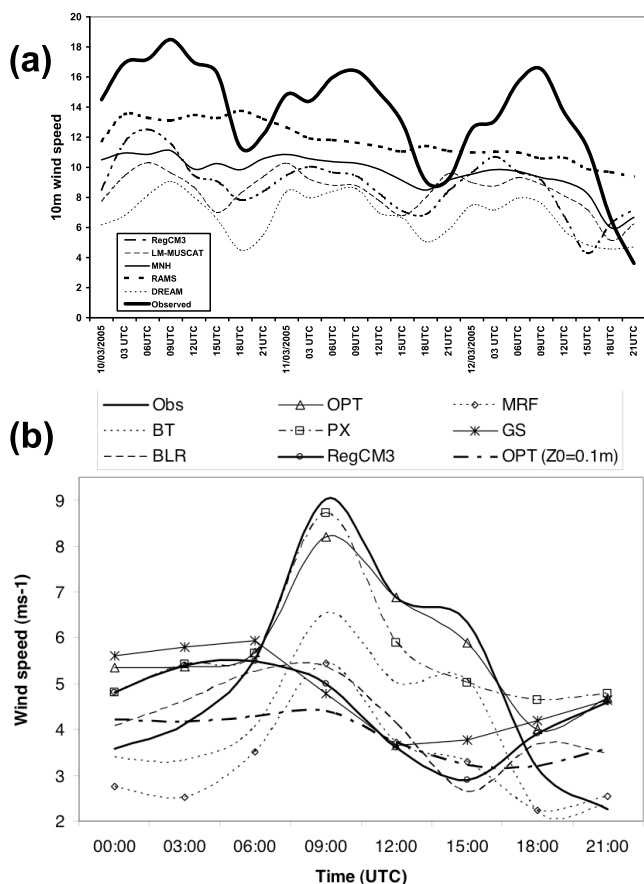
Figure 8. Modeling low-level jets and associated surface winds over the Bodélé Depression. (a) Comparison between observations (solid line) and simulations with five different regional models (horizontal resolutions between 7 and 26 km [*Todd et al.*, 2008a, Figure 4]). Most models tend to underestimate the diurnal cycle and the absolute magnitude of the winds. (b) Mean diurnal cycle in observations (solid) and simulations with the same model in different PBL configurations [*Todd et al.*, 2008b Figure 7a]. Different PBL representations can lead to large differences in wind magnitude and diurnal cycle. Figure 8b is © American Meteorological Society. Reprinted with permission.

This type of event is most frequent during spring, when the baroclinicity along the Mediterranean coast is maximized and supports cyclone intensification [*Alpert and Ziv*, 1989]. Figure 9b shows an example of a Khamsin cyclone with its core over Turkey, which caused widespread dust emission over Libya and Egypt. The dust emitted by Khamsin cyclones often gets carried over the Mediterranean Sea and sometimes even into Europe with the southerly winds ahead of the system.

[42] Second, ridging of the subtropical high increases the south-north pressure gradient over the Sahara and leads to a surge in the northeasterly harmattan or Etesian winds with strong effects on the central and southern Sahara and the Sahel [*Washington and Todd*, 2005; *Knippertz and Fink*, 2006; *Knippertz et al.*, 2011]. Examples for this type of situation include an intensified Libyan high associated with dust outbreaks from the Bodélé Depression [*Washington*

and Todd, 2005; *Washington et al.*, 2006] (Figure 10) as well as an intensified and southeastward extended Azores high activating dust sources in Mauritania, Mali, and Algeria [*Knippertz et al.*, 2011]. In both cases, dust emission and surface winds show a clear diurnal cycle affected by the formation of LLJs (see section 3.2.1). Long-lasting, extensive events with high dust amounts are often associated with explosive anticyclogenesis behind a surface cold front penetrating into the northern Sahara. Prominent examples of this type, which generated considerable research interest, occurred during 2–7 March 2004 [*Knippertz and Fink*, 2006; *Min et al.*, 2009; *Mangold et al.*, 2011; *Shao et al.*, 2010] and 7–13 March 2006 [*Slingo et al.*, 2006; *Tulet et al.*, 2008; *Cavazos et al.*, 2009; *Mallet et al.*, 2009; *Stanelle et al.*, 2010]. The evaporating precipitation along the cold front can play an important role in the early stages of these events [*Knippertz and Fink*, 2006]. Generally, numerical models satisfactorily reproduce such large-scale dust outbreaks [*Cavazos et al.*, 2009; *Shao et al.*, 2010] (Figure 11) in that the meteorological drivers of emission and transport provide accurate depiction of timing/transport of dust and AOT with respect to satellite observations. Indeed, in the study of *Cavazos et al.* [2009], model dust estimate errors are dominated by poor representation of specific local sources as a result of inadequate soil information.

[43] In summer, there is a large background pressure gradient into the SHL (Figure 1b), which frequently generates high surface winds, often associated with LLJ formation. This is particularly true for the dry northerly, westerly, and easterly inflow [*Knippertz*, 2008; *Grams et al.*, 2010]. On the moist side of the "intertropical discontinuity" (ITD), which separates Saharan and tropical air masses over Africa, surface inversions are weaker, leading to less decoupling and LLJ formation (see section 3.2.1). Nevertheless, the often large monsoon pressure gradient allows a substantial acceleration of the near-surface wind in stable conditions during the night [*Parker et al.*, 2005], which can lead to dust emissions near the leading edge of the monsoon flow [*Flamant et al.*, 2007; *Bou Karam et al.*, 2008], possibly associated with intermittent LLJ mixing events. The example north-south lidar transect across southern West Africa shown in Figure 12 indicates two regions of dust uplift within the northward progressing monsoon flow. One is the actual leading edge of the monsoonal air; the southern one has been speculated to be the remnants of a convective cold pool (see section 3.2.2) [see also *Marsham et al.*, 2008a]. Rather little is known about the vertical wind structure of these events. The representation of this feature in numerical models has not been systematically investigated but will be closely linked to the representation of the monsoon circulation, which is a large challenge for many coarse-resolution models [*Cook and Vizy*, 2006; *Marsham et al.*, 2011].

[44] The dominant synoptic scale weather systems over summertime West Africa are African easterly waves (AEWs). It has long been known that AEWs modify dust transport over the tropical Atlantic [*Karyampudi and Carlson*, 1988; *Westphal et al.*, 1988], but their role for the dust distribution over the continent is less clear. Recently,
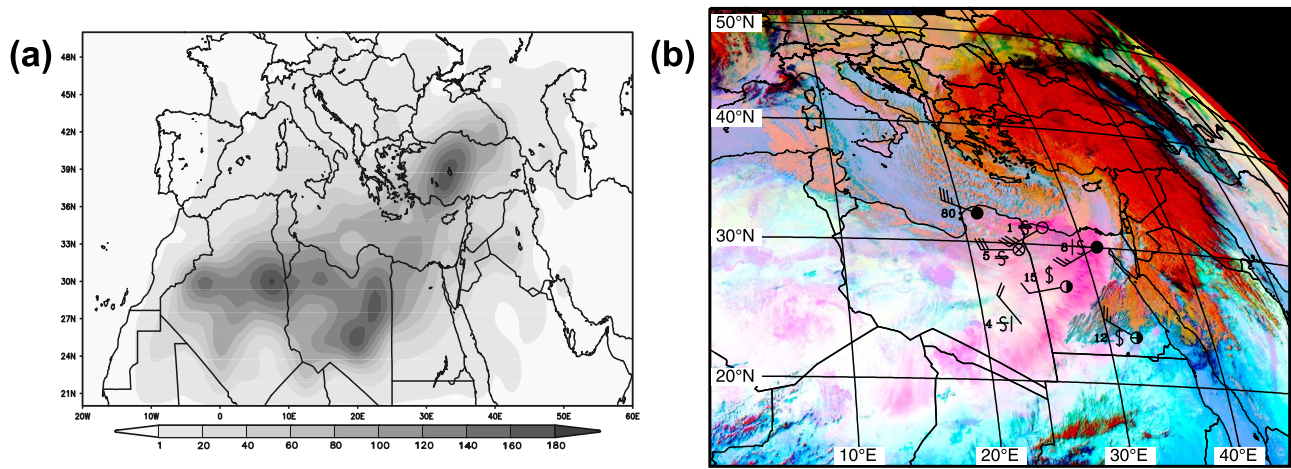
Figure 9. Characteristic synoptic scale weather system associated with dust emission: the Saharan cyclone. (a) Climatology of Saharan cyclone counts in 2.5° × 2.5° grid boxes for March–May 1958–2006 showing maximum activity across the Algerian and Libyan Sahara [*Hannachi et al.*, 2010, Figure 6]. With kind permission from Springer Science + Business Media. (b) Example of a Saharan cyclone on 22 January 2004 in the SEVIRI dust product overlaid with synoptic station reports from Libya and Egypt. The dark red colors show the main cloud mass of the cyclone and cold front, while pink colors indicate dust emission behind the front (also see the Figure 3 caption).

Knippertz and Todd [2010] suggested that AEWs contribute to the synoptic scale variability of the WS hot spot through (1) the organization of dust transport, (2) dust emission around the AEW surface vortex if it is strong enough, and (3) dust emission in connection with convective cold pools (see section 3.2.2) forming in the moist southerlies to the east of the AEW trough upstream of the WS (Figure 13).

The same authors provide evidence that interactions between AEWs and subtropical upper level troughs play a role in creating extended areas of southerly moisture advection into the Sahara and northerly dust advection into the WS. Such interactions have been proposed to create dust-generating, traveling surface disturbances called Soudano-Saharan Depressions, but this concept has recently been questioned
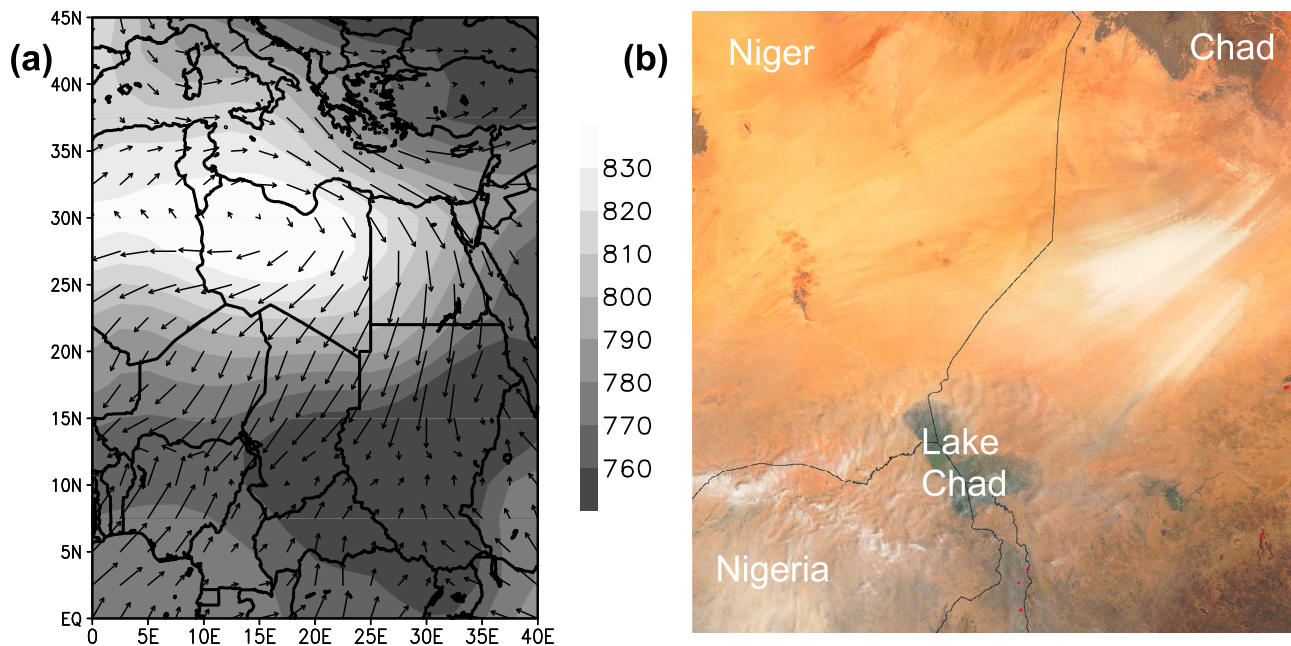

Figure 10. Characteristic synoptic scale weather system associated with dust emission: ridging of subtropical high. (a) Composite mean geopotential height at 925 hPa (geopotential meters, shading) and wind vectors (m s^{-1}) for 10–12 March 2005 associated with dust outbreaks from the Bodélé Depression in Chad. The strong anticyclone over Libya increases the north-south pressure gradient and causes a surge in the northeasterly harmattan flow [*Todd et al.*, 2008a, Figure 2b]. (b) Visible satellite image of a Bodélé Depression dust outbreak [*Washington and Todd*, 2005, Figure 1].
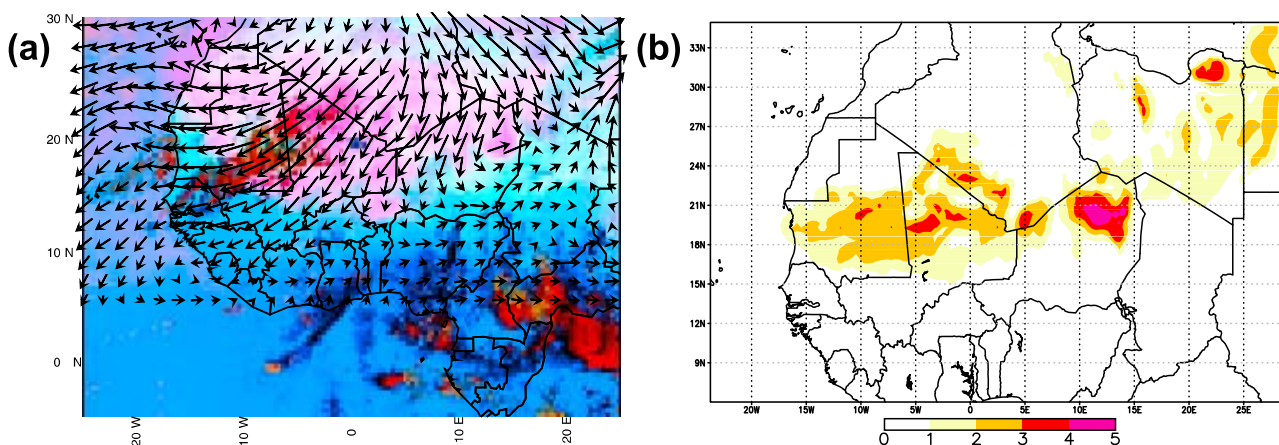
Figure 11. Characteristic synoptic scale weather system associated with dust emission: explosive anticyclogenesis. (a) SEVIRI false color dust composite at 1200 UTC 7 March 2006 (see the Figure 3 caption for explanation) overlain with 925 hPa winds from a regional climate model version 3 (RegCM3) simulation. (b) Corresponding AOT from the same model simulation showing good qualitative agreement with the observations. Figures 11a and 11b are from *Cavazos et al.* [2009, Figure 3].

on the basis of modern reanalysis and satellite data [*Schepanski and Knippertz*, 2011]. AEWs are reasonably well represented in state-of-the-art weather prediction models, although interactions with moist convection and the land surface can lead to errors in both strength and propagation [*Sander and Jones*, 2008; *Shen et al.*, 2010]. Systematic evaluation of model representation of tropical-temperate interactions over the Sahara in relations to these specific synoptic scale features has yet to be conducted.

3.2.3. Mesoscale

[45] A prominent dust storm type on scales of several hundred kilometers is the so-called "haboob," which is caused by evaporationally driven, cold near-surface outflow from organized moist convection. In particular, the squall lines of the Sahel have long been connected to this kind of dust storm [*Sutton*, 1925; *Farquharson*, 1937; *Freeman*, 1952]. The strong gust winds at the leading edge of the cold pool can lead to dramatic moving "walls of dust" (Figure 14a) and very sharp increases in wind speed and particle concentrations (Figure 14b). Haboobs have been documented for the northern [*Knippertz et al.*, 2007; *Emmel et al.*, 2010] and southern margins of the Sahara [*Lawson*, 1971; *Marsham et al.*, 2008a; *Williams et al.*, 2008; *Knippertz and Todd*, 2010] and other deserts worldwide [*Idso et al.*, 1972; *Membery*, 1985; *Chen and Fryrear*, 2002; *Takemi*, 2005; *Miller et al.*, 2008]. Because of the diurnal cycle of deep moist convection haboobs tend to cluster in the late afternoon until early morning [*Emmel et al.*, 2010]. There is an ongoing debate in the scientific community on how much haboobs contribute to total dust emission, partly caused by the difficulties of satellites to detect dust underneath convective cloud shields and problems in distinguishing and tracking specific events [*Engelstaedter and Washington*, 2008; *Williams*, 2008]. Another aspect of debate is subsequent wet deposition of dust particles by convective rains, but SEVIRI dust imagery has recently revealed that at least the northern parts of many large dusty

cold pools can move sufficiently far away from the precipitation area (see *Knippertz and Todd* [2010] for examples). Figure 14d shows a CALIOP lidar cross section through the cold pool of an extended haboob penetrating from Niger into southern Algeria (Figure 14c). The sharp, inclined leading edge is clearly visible in the lidar profile connecting with an elevated dust layer from the previous day further south. Their enormous spatial scale and vigor make haboobs one of the most spectacular features in dust research.

[46] Modeling haboobs is a great challenge closely tied to a realistic representation of organized moist convection with a clear dependence on horizontal resolution and convection parameterization [*Knippertz et al.*, 2009a; *Reinfried et al.*, 2009; C. Cavazos and M. C. Todd, Model simulations of a complex dust event over the Sahara during the West African monsoon onset, submitted to *Advances in Meteorology*, 2011] (Figures 14e and 14f). Recent results by *Marsham et al.* [2011] have shown that the contribution from
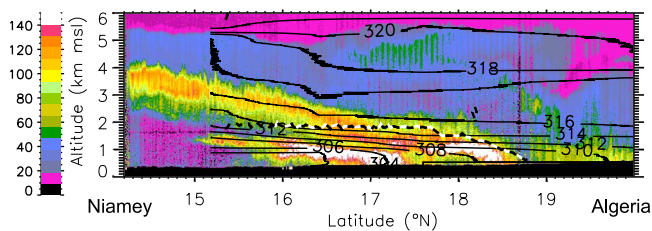

Figure 12. Characteristic summertime dust emission process: the monsoon nocturnal surge. Airborne lidar-derived atmospheric reflectivity at 732 nm along a vertical cross section between Niamey (Niger) and southern Algeria observed during the AMMA special observation period 2 peak monsoon (0602–0658 UTC 7 July 2006) [*Bou Karam et al.*, 2008, Figure 7]. The high reflectivity between 18°N and 19°N marks the leading edge of the southwesterly monsoon flow that accelerates in the course of the night. The black lines are lines of constant potential temperature indicating the stable stratification in the early morning hours.
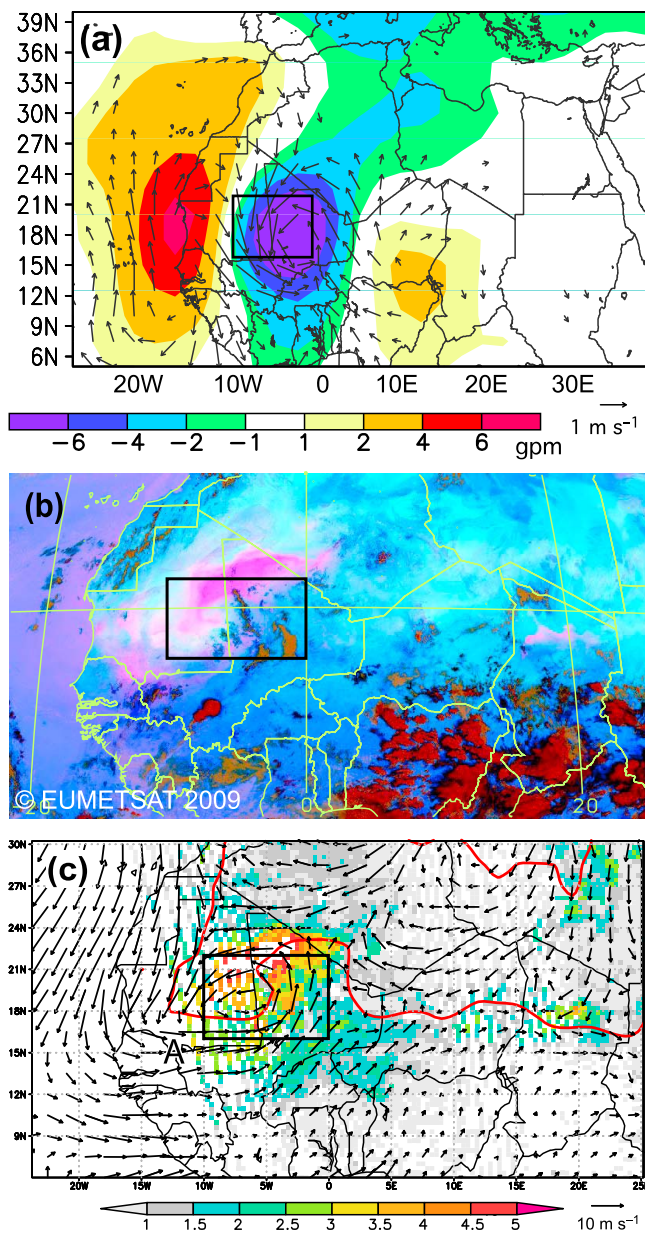
Figure 13. Characteristic summertime dust emission processes: the synoptic scale surface trough. (a) Mean sea level pressure and 925 hPa wind anomalies associated with large positive perturbations in TOMS *AI* over the western Sahara (black box in all figures) during June–September 1979–1993. The patterns indicate enhanced cyclonic winds in the area of the surface trough of an African easterly wave during dust events. (b) SEVIRI dust product (see the Figure 3 caption for explanation) for an example case on 18 July 2006 showing a marked dust plume over the western Sahara. (c) OMI *AI* (shading), 925h Pa winds (vectors), and the intertropical discontinuity (red line) for the same time. Strongest dust signals occur in the northeasterly flow around the cyclonic center and are associated with convection and haboob dust events in the southerly flow [*Knippertz and Todd*, 2010, Figures 4g, 5c, and 5d].

haboob dust emission changes dramatically between simulations using the same model with and without convective parameterization. There are examples of large haboobs over the Sahara, which are not even represented in analysis data because of a lack of observations and difficulties with getting the model to generate the parent convection [*Knippertz et al.*, 2009b]. The key problem is that convective parameterizations are designed to release convective instability within a model grid box and therefore do not allow for the spatial separation of the up- and downdrafts that are crucial to the mesoscale organization and the formation of cold pools, which in reality can easily reach dimensions of many grid boxes of a typical regional model as shown by Figures 14c–14f. Another issue is the correct initiation of convection in the model, which is sensitive to surface topography and soil moisture heterogeneity [*Taylor et al.*, 2011]. Moist convection can also be associated with very small-scale and short-lived intense wind events, sometimes referred to as "dry microbursts" [*Wakimoto*, 2001]. These can be expected to cause dust emission too, but there is very limited research on this topic so far. These results, in particular, those of *Marsham et al.* [2011], suggest that an important dust emission mechanism is not satisfactory represented in the majority of dust models, which has important ramifications on the diurnal cycle and the activation of source regions in the Sahel, where haboobs are most common. There is a need to better quantify the contribution of haboobs to dust emission, transport, and deposition and to explore cost-effective ways to better represent their impacts in models.

3.2.4. Microscale

[47] On scales of a few to several hundred meters, turbulent circulations in the dry convective daytime PBL over deserts can cause considerable emission over bare dry lands on days with high insolation and weak background winds [*Sinclair*, 1969; *Ansmann et al.*, 2009b]. These can take the form of more compact rotating dust devils and larger, longer-lived nonrotating dusty plumes [e.g., *Koch and Renno*, 2005]. There are relatively few high-quality observations of these features over the Sahara. Satellite data is clearly too coarse to monitor microscale systems and in situ measurements are challenging because of logistics. Figure 15a shows lidar measurements from summertime southern Morocco, which give a good indication of the frequency and depths of dusty plumes that stand out as areas of high depolarization (red colors). Clearly identifiable plumes occur on timescales of 10–30 min. Maximum depth increases in the course of the morning reaching values of up to 2 km above the ground (3 km above sea level) around midday.

[48] The contribution of dust devils and dusty plumes to the global dust emission is unknown, but extrapolations of limited observations in North America suggest values of up to 35% [*Koch and Renno*, 2005]. The applicability of these measurements to the Sahara, however, is not clear because of differences in land surface and PBL characteristics and most evidence from satellite data and field campaigns suggests that synoptic and mesoscale processes dominate. The increase in computer capacities in recent years has made it
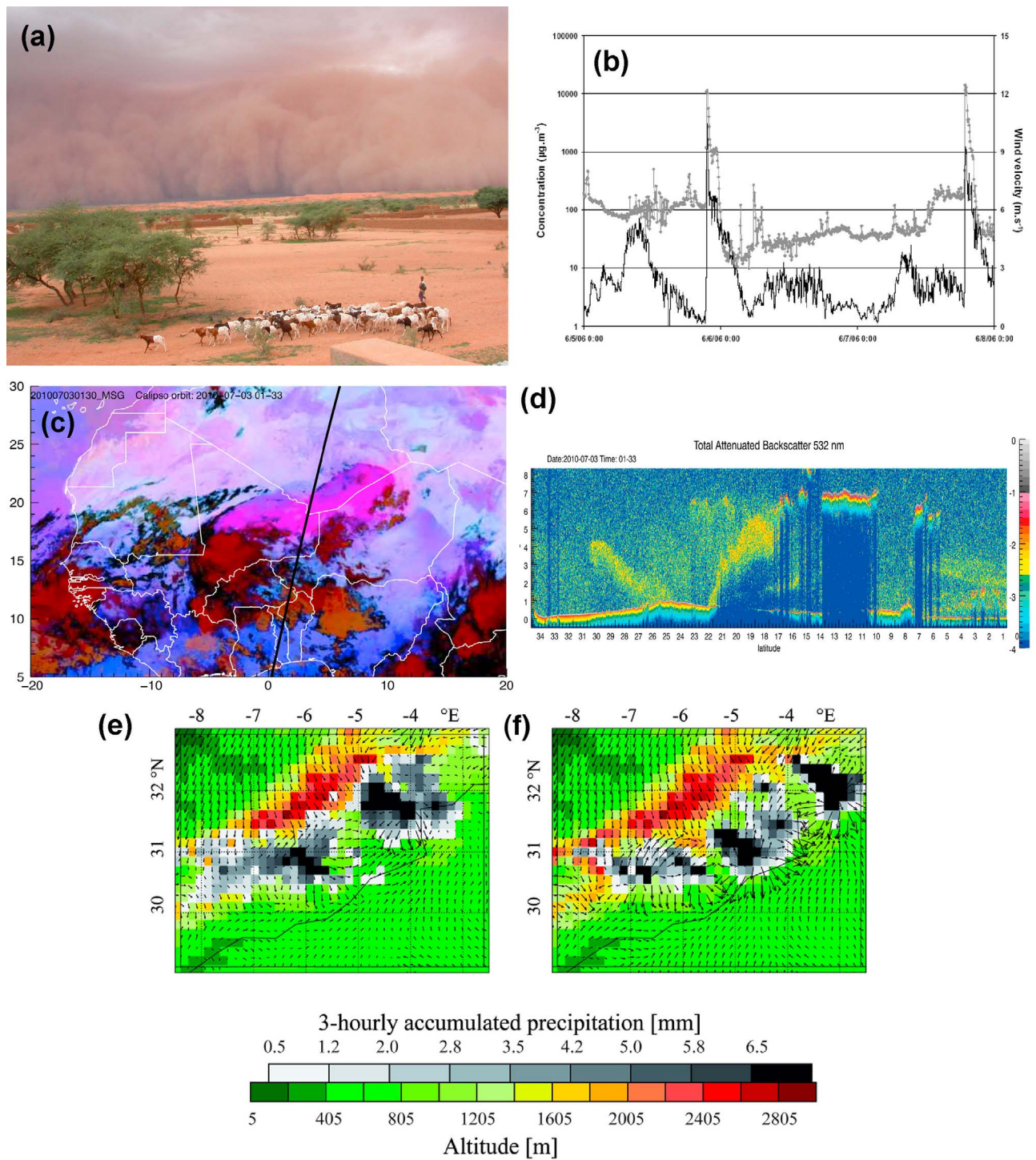
Figure 14. Characteristic summertime dust emission process: haboobs. (a) Photograph of the leading edge of a haboob in Hombori, Mali (photo courtesy of Françoise Guichard, CNRS Photothèque). (b) Surface measurements of PM$_{10}$ concentrations and wind speed at Cinzana (Mali) showing the passage of two haboobs during 5–7 June 2006 [*Marticorena et al.*, 2010, Figure 15]. View from space of a haboob around 0130 UTC 3 July 2010 showing (c) MSG SEVIRI and (d) CALIOP data as in Figure 3. Going south to north the CALIOP section shows altocumulus clouds over southern West Africa, elevated dust from the previous day around 17°N, the sharp inclined leading edge of the haboob, and possibly dust gliding onto cooler Mediterranean air in the north. (e and f) Simulations of a haboob near the High Atlas in Morocco on 3 June 2006. Shown are model topography, 10 m winds, and precipitation. While the simulation using 7 km grid spacing and the Kain-Fritsch convection scheme (Figure 14e) struggles to reproduce the event, a 2.8 km simulation with explicit deep convection (Figure 14f) performs much better [*Reinfried et al.*, 2009, Figure 8].
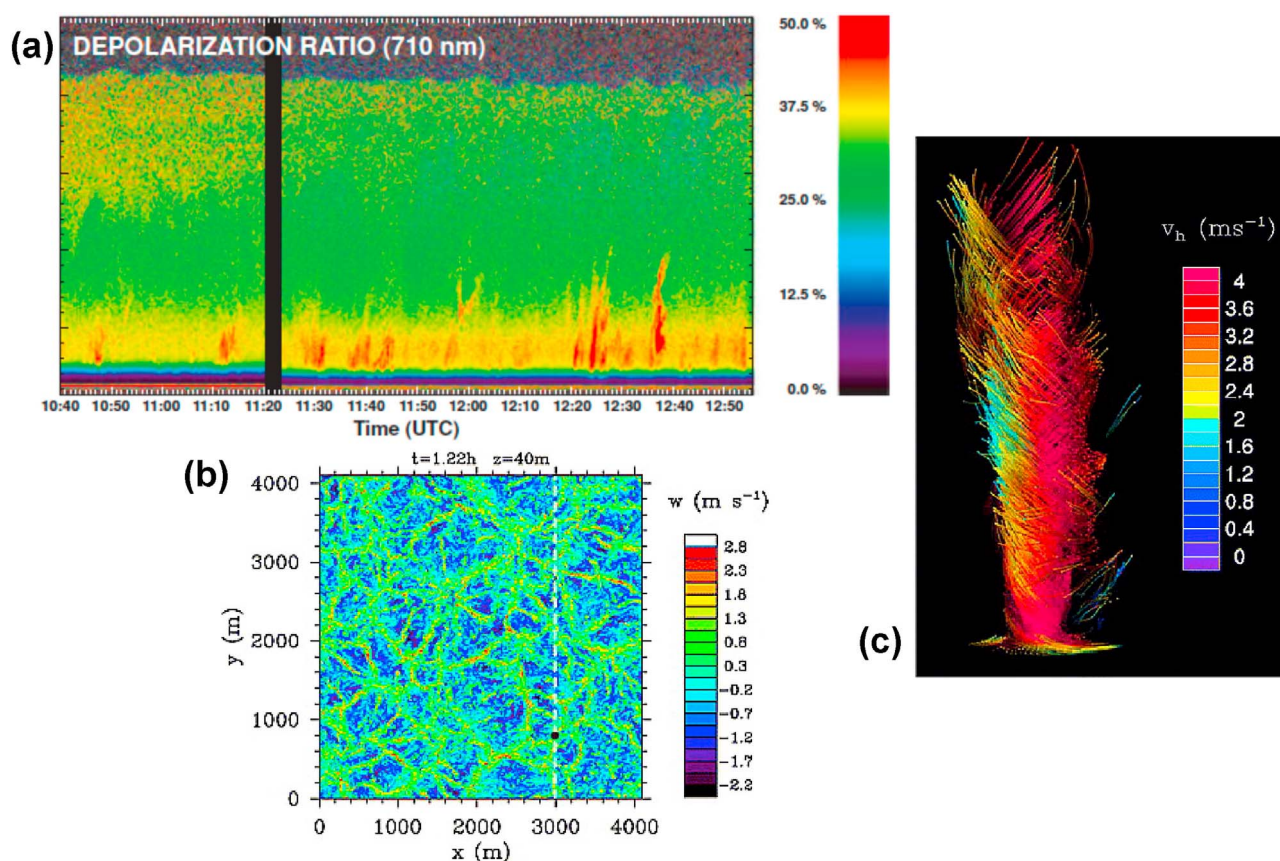
Figure 15. Microscale emission processes. (a) Observations of dusty plumes by lidar taken on 16 May 2006 between 1040 and 1258 UTC in Ouarzazate, southern Morocco, during SAMUM-1. The dust plumes stand out as regions of high depolarization reaching up to 2 km above ground level [*Ansmann et al.*, 2009b, Figure 2]. (b) High-resolution large eddy simulations of dry convection in an active daytime desert boundary layer with a forming dust devil marked by a black dot. Shown is vertical motion at 40 m above ground. (c) Flow visualization using trajectories with colors showing horizontal wind speed [from *Raasch and Franke*, 2011, Figures 2 and 11].

possible to generate idealized large eddy simulations of dust devils with resolutions down to a few meters for research purposes [*Kanak*, 2005; *Ohno and Takemi*, 2010; *Raasch and Franke*, 2011; *Sullivan and Patton*, 2011]. An example from such a conceptual simulation is shown in Figure 15b. The structure of vertical motions at 40 m above ground indicates PBL eddies bounded by areas of strong uplift. The associated horizontal convergence at the surface is most likely associated with dusty plumes in the more intense regions. In addition, the model shows the formation of a rotating dust devil at the intersection of several uplift branches (marked by a black dot). Theoretical, observational, and modeling studies show that dust devils are sensitive to sensible heat flux, background wind, and PBL depth [*Rennó et al.*, 1998]. The effects of dust devils are not considered in dust models so far and are unlikely to be reflected in TKE approaches as the one by *Cakmur et al.* [2004] (see end of section 2.3.1), as these assume isotropic eddies in the PBL.

3.2.5. Vertical Dust Transport

[49] As described in section 3.1.3, the summertime vertical structure of the dust distribution is complex. Recent measurements have revealed a variety of dynamical control mechanisms for mixing and transport. These are summarized by *Cuesta et al.* [2009] and schematically depicted in Figure 6. Dust emitted over the Sahara (most often in the hours after sunrise, see section 3.1.2) will be mixed vertically through the Saharan convective boundary layer (SCBL). This occurs most strongly during the hot summer season when observations reveal that the SCBL extends up to ~5–6 km across a vast extent of the central Sahara north of the ITD (Feature I in Figure 6). Dust is typically well mixed throughout this layer within a day or two of emission as exemplified in Figure 3.

[50] Dynamical lifting occurs when cooler air intrudes into the Sahara most commonly along the ITD where the monsoon flow undercuts the SAL or when midlatitude weather systems advect cooler air from the Atlantic sector (Features II.b and II.a, respectively, in Figure 6). The resulting slanting isentropes cause an upgliding of the dusty SAL over the monsoon or midlatitude air. The elevated SAL is clearly visible as a ubiquitous feature in CALIOP lidar profiles south of the ITD (Figure 3). Further, more detailed features in the vertical structure of the SCBL are associated with the

effects of topography and surface albedo patterns. Horizontal flow over and around major topographic barriers (e.g., the Hoggar and Tibesti Mountains) can induce variations in wind speed and in the depth of the SCBL (a hydraulic "jump") downwind of mountains [e.g., *Drobinski et al.*, 2005] (Features II.a and II.b in Figure 6). Localized heating over regions of low albedo associated with particular geological features and mountains can result in hot spots driving deeper convection during daytime (Features III.c and III.d, respectively, in Figure 6). This has implication for vertical mixing in those areas and for the compensating circulation and vertical structure of the SCBL in the surrounding areas [*Marsham et al.*, 2008b].

[51] Fine detail on the vertical structure of dust was provided by lidar observations during SAMUM-1 in southern Morocco, providing the first surface lidar observations of the full diurnal cycle of dust transport and mixing. These observations have shown that during stable nighttime conditions differential advection can lead to complicated layering in the lowest ~5 km of the atmosphere, which are then mixed vertically in the course of the following day [*Knippertz et al.*, 2009b]. The different layers can be separated by weak lids, which are often poorly resolved in numerical models because of insufficient vertical resolution. This can cause a too early mixing of air from difference layers. Similarly, simulations of summertime dust events with the Weather Research and Forecasting (WRF) regional model reveal that too weak inversions at the SCBL top allow dust to be mixed to excessive heights (Cavazos and Todd, submitted manuscript, 2011).

4. CONCLUSIONS AND FUTURE DIRECTIONS

[52] Mineral dust aerosol is an important component of the Earth system and efforts to incorporate the effects of dust in weather and climate models is at the cutting edge of the discipline. The Sahara desert is by far the world's dominant dust source with implications for the local, regional, and global climate. This paper summarizes the advances made in recent years in our understanding of mineral dust processes over the Sahara, emerging primarily from analysis of (1) new satellite observations, (2) intensive field and airborne observational campaigns, and (3) high-resolution regional model simulations. The emphasis here is specifically on the meteorological processes of dust emission and transport. What has emerged from this research is (1) a greatly improved quantitative representation of the 4-D structure of Saharan dust plumes, (2) a more complete list of the multiscale meteorological processes responsible, and (3) a deeper understanding of the utility and key limitations of models in representing these processes.

[53] There are fundamental differences between the winter and summer conditions. The former is characterized more by synoptic scale processes and often dry dynamics leading to episodic strong dust events affecting mostly the lowest 1.5 km of the atmosphere. Cyclonic storms in the northern Sahara and surges in the harmattan or Etesian winds farther south associated with a pulsing of subtropical high-pressure

systems are dominating. The summertime is more complex involving a wider range of sources and mechanisms, leading to a much deeper dust layer that frequently gets elevated when advected over cooler air surrounding the Sahara. Important meteorological features include AEWs and interactions with midlatitude troughs, the SHL, the monsoon circulation, haboobs, and dust devils and dusty plumes in the dry convective PBL. Nocturnal LLJs are common during both winter and summer and are an important control on diurnal variations in dust distribution.

[54] We can identify a number of critical challenges that should be addressed in future research substantially associated with the representation of peak winds.

[55] 1. The role of moist convective processes and cloud/precipitation systems is clearly central to dust emission, transport, and deposition in the Sahara and the Sahel during summer, most vividly expressed through the dramatic haboob dust events. However, even regional models running at grid spacings as low at 10 km do not adequately represent these processes, neither in climatological terms nor for weather forecasting. Addressing this is especially problematic as it requires improvements both in models and in detailed observations of aerosols under cloud systems, which is not currently possible from any of the satellite or ground-based observational systems. Representing moist convective processes has long been recognized as a challenge to models and was part of the rationale for the AMMA and other campaigns. However, the overwhelming emphasis in previous research has understandably been on representing precipitation processes and there is a clear need for a focused effort to observe and simulate the extreme wind events associated with moist convective processes.

[56] 2. The role of dry convective processes in the PBL on dust emission and mixing. There are two components to this. First, the contribution of dry convective eddies (dust devils) to dust emission remains essentially unknown. During summer, in particular, the deep SAL has a high background aerosol load. It is not clear to what extent this is the result of mixing and transport of dust from episodic synoptic and mesoscale events or from microscale dust devil–like processes. The latter are not at all well observed from satellite and existing surface observations over the Sahara are not adequate to resolve them. The "Fennec" project, combining detailed surface observations and high-resolution, eddy-resolving modeling, should provide valuable insights in this regard. Second, while the LLJ features have been highlighted as central to dust emission and transport, there remain substantial uncertainties in model representation of LLJs through inadequate handling of the fine detail of the nocturnal stable PBL as well as the downward mixing of LLJ momentum during the buildup of the PBL in the morning. The timing and height of vertical mixing of dust during the day is controlled by often subtle layering in the atmosphere, which models struggle to resolve. In addition, there remains the problem of a lack of detailed information on land surface characteristics (soil texture, moisture, roughness, and land cover characteristics) and its temporal variations, required by physically based emission schemes.

[57] Addressing these challenges requires a combination of (1) more extensive, fine-grained observational programs, such as the recent Fennec field campaign; (2) further advances in satellite retrievals with high-resolution modeling; (3) more thorough testing, evaluation, and sensitivity studies of model parameterization of meteorological processes (e.g., PBL, convection, and microphysics schemes) and dust processes (emission and deposition); and (4) a concerted effort to develop model parameterizations specifically tested for the unique conditions of the Sahara desert. The last is the goal of the recently started "Desert Storms" project at the University of Leeds (http://www.see. leeds.ac.uk/research/icas/working-groups/knippertz/projects/ desert-storms/). Representing subgrid-scale wind variability through probability density functions on the basis of measures of turbulence [*Cakmur et al.*, 2004] is a promising general concept that will be followed in this project. This approach, however, is of limited advantage if the process generating the turbulence (the LLJ or its breakdown, the haboobs, the dust devil, etc.) is not satisfactorily represented in the model in the first place, calling for further parameterization efforts on the level of single meteorological processes involved in peak wind generation. We expect that for the time being, dust modeling will have to rely on some degree of tuning to account for the lack of high-resolution soil information, but that the new insights gained in recent years will lead the way to a more physical representation of smaller-scale meteorological processes that will ultimately improve geographical variations, vertical structure, seasonality, and the diurnal cycle of the dust distribution in models as well as short-term forecasts of dust hazards and air quality.

[59] The Editor responsible for this paper was Greg Okin. He thanks Beatrice Marticorena and two anonymous reviewers.

REFERENCES

Alfaro, S. C., and L. Gomes (2001), Modeling mineral aerosol production by wind erosion: Emission intensities and aerosol size distributions in source areas, *J. Geophys. Res.*, *106*(D16), 18,075–18,084, doi:10.1029/2000JD900339.

Alfaro, S., A. Gaudichet, L. Gomes, and M. Maillé (1998), Mineral aerosol production by wind erosion: Aerosol particle sizes and binding energies, *Geophys. Res. Lett.*, *25*, 991–994, doi:10.1029/98GL00502.

Alpert, P., and B. Ziv (1989), The Sharav cyclone: Observations and some theoretical considerations, *J. Geophys. Res.*, *94*(D15), 18,495–18,514, doi:10.1029/JD094iD15p18495.

Ansmann, A., H. Baars, M. Tesche, D. Muller, D. Althausen, R. Engelmann, T. Pauliquevis, and P. Artaxo (2009a), Dust and smoke transport from Africa to South America: Lidar profiling over Cape Verde and the Amazon rainforest, *Geophys. Res. Lett.*, *36*, L11802, doi:10.1029/2009GL037923.

Ansmann, A., M. Tesche, P. Knippertz, E. Bierwirth, D. Althausen, D. Müller, and O. Schulz (2009b), Vertical profiling of convective dust plumes in southern Morocco during SAMUM, *Tellus B*, *61*, 340–353, doi:10.1111/j.1600-0889.2008.00384.x.

Ansmann, A., A. Petzold, K. Kandler, I. Tegen, M. Wendisch, D. Müller, B. Weinzierl, T. Müller, and J. Heintzenberg (2011), Saharan Mineral Dust Experiments SAMUM-1 and SAMUM-2: What have we learned?, *Tellus B*, *63*, 403–429, doi:10.1111/j.1600-0889.2011.00555.x.

Bagnold, R. A. (1935), The movement of desert sand, *Geogr. J.*, *85*(4), 342–365, doi:10.2307/1785593.

Bagnold, R. A. (1937), The transport of sand by wind, *Geogr. J.*, *89*(5), 409–438, doi:10.2307/1786411.

Banta, R. M., Y. L. Pichugina, and R. K. Newsom (2003), Relationship between low-level jet properties and turbulence kinetic energy in the nocturnal stable boundary layer, *J. Atmos. Sci.*, *60*, 2549–2555, doi:10.1175/1520-0469(2003)060<2549:RBLJPA>2.0.CO;2.

Ben-Ami, Y., I. Koren, Y. Rudic, P. Artaxo, S. T. Martin, and M. O. Andreae (2010), Transport of North African dust from the Bodélé Depression to the Amazon Basin: A case study, *Atmos. Chem. Phys.*, *10*, 7533–7544, doi:10.5194/acp-10-7533-2010.

Ben-Ami, Y., I. Koren, O. Altaratz, A. B. Kostinski, and Y. Lehahn (2011), Discernible rhythm in the spatio/temporal distributions of transatlantic dust, *Atmos. Chem. Phys. Discuss.*, *11*, 23,513–23,539, doi:10.5194/acpd-11-23513-2011.

Biasutti, M., A. H. Sobel, and S. J. Camargo (2009), The role of the Sahara Low in Sahel rainfall variability and change in the CMIP3 models, *J. Clim.*, *22*, 5755–5771, doi:10.1175/2009JCLI2969.1.

Blackadar, A. K. (1957), Boundary layer wind maxima and their significance for the growth of nocturnal inversions, *Bull. Am. Meteorol. Soc.*, *38*, 282–290.

Bou Karam, D., C. Flamant, P. Knippertz, O. Reitebuch, J. Pelon, M. Chong, and A. Dabas (2008), Dust emissions over the Sahel associated with the West African monsoon intertropical discontinuity region: A representative case study, *Q. J. R. Meteorol. Soc.*, *134*, 621–634, doi:10.1002/qj.244.

Bou Karam, D., C. Flamant, J. Cuesta, J. Pelon, and E. Williams (2010), Dust emission and transport associated with a Saharan depression: The February 2007 case, *J. Geophys. Res.*, *115*, D00H27, doi:10.1029/2009JD012390.

Brindley, H., and A. Ignatov (2006), Retrieval of mineral aerosol optical depth and size information from Meteosat Second Generation solar reflectance bands, *Remote Sens. Environ.*, *102*, 344–363, doi:10.1016/j.rse.2006.02.024.

Bristow, C. S., K. A. Hudson-Edwards, and A. Chappell (2010), Fertilizing the Amazon and equatorial Atlantic with West African dust, *Geophys. Res. Lett.*, *37*, L14807, doi:10.1029/2010GL043486.

Cakmur, R. V., R. L. Miller, and O. Torres (2004), Incorporating the effect of small-scale circulations upon dust emission in an atmospheric general circulation model, *J. Geophys. Res.*, *109*, D07201, doi:10.1029/2003JD004067.

Cakmur, R. V., R. L. Miller, J. Perlwitz, I. V. Geogdzhayev, P. Ginoux, D. Koch, K. E. Kohfeld, I. Tegen, and C. S. Zender (2006), Constraining the magnitude of the global dust cycle by minimizing the difference between a model and observations, *J. Geophys. Res.*, *111*, D06207, doi:10.1029/2005JD005791.

Carboni, E., G. Thomas, R. Grainger, C. Poulsen, R. Siddans, D. Peters, E. Campmany, A. Sayer, and H. Brindley (2007), Retrieval of aerosol properties from SEVIRI using visible and infrared channels, paper presented at Joint 2007 EUMETSAT/AMS Conference, Amsterdam, 24–28 Sep.

Carboni, E., et al. (2009), Desert-dust satellite retrieval intercomparison, *Geophys. Res. Abs.*, *11*, Abstract EGU2009-0.

Carlson, T. N., and J. M. Prospero (1972), The large-scale movement of Saharan air outbreaks over the northern equatorial Atlantic, *J. Appl. Meteorol.*, *11*, 283–297, doi:10.1175/1520-0450(1972)011<0283:TLSMOS>2.0.CO;2.

Cavalieri, O., et al. (2010), Variability of aerosol vertical distribution in the Sahel, *Atmos. Chem. Phys.*, *10*, 12,005–12,023, doi:10.5194/acp-10-12005-2010.

Cavazos, C., M. C. Todd, and K. Schepanski (2009), Numerical model simulation of the Saharan dust event of 6–11 March 2006 using the regional climate model version 3(RegCM3), *J. Geophys. Res.*, *114*, D12109, doi:10.1029/2008JD011078.

Chaboureau, J.-P., P. Tulet, and C. Mari (2007), Diurnal cycle of dust and cirrus over West Africa as seen from Meteosat Second Generation satellite and a regional forecast model, *Geophys. Res. Lett.*, *34*, L02822, doi:10.1029/2006GL027771.

Chen, W., and D. Fryrear (2002), Sedimentary characteristics of a haboob dust storm, *Atmos. Res.*, *61*, 75–85, doi:10.1016/S0169-8095(01)00092-8.

Chiapello, I., G. Bergametti, L. Gomes, B. Chatenet, F. Dulac, J. Pimenta, and E. S. Suares (1995), An additional low layer transport of Sahelian and Saharan dust over the northeastern tropical Atlantic, *Geophys. Res. Lett.*, *22*, 3191–3194, doi:10.1029/95GL03313.

Christopher, S. A., P. Gupta, B. Johnson, C. Ansell, H. Brindley, and J. Hawood (2011), Multi-sensor satellite remote sensing of dust aerosols over North Africa during GERBILS, *Q. J. R. Meteorol. Soc.*, *137*, 1168–1178, doi:10.1002/qj.863.

Cook, K. H., and E. K. Vizy (2006), Coupled model simulations of the West African monsoon system: Twentieth- and twenty-first-century simulations, *J. Clim.*, *19*, 3681–3703, doi:10.1175/JCLI3814.1.

Cuesta, J., J. H. Marsham, D. J. Parker, and C. Flamant (2009), Dynamical mechanisms controlling the vertical redistribution of dust and the thermodynamic structure of the west Saharan atmospheric boundary layer during summer, *Atmos. Sci. Lett.*, *10*, 34–42, doi:10.1002/asl.207.

Darmenova, K., I. N. Sokolik, Y. Shao, B. Marticorena, and G. Bergametti (2009), Development of a physically based dust emission module within the Weather Research and Forecasting (WRF) model: Assessment of dust emission parameterizations and input parameters for source regions in central and East Asia, *J. Geophys. Res.*, *114*, D14201, doi:10.1029/2008JD011236.

de Reus, M., F. Dentener, A. Thomas, S. Borrmann, J. Ström, and J. Lelieveld (2000), Airborne observations of dust aerosol over the North Atlantic Ocean during ACE 2: Indications for heterogeneous ozone destruction, *J. Geophys. Res.*, *105*(D12), 15,263–15,275, doi:10.1029/2000JD900164.

Desboeufs, K. V., and G. Cautenet (2005), Transport and mixing zone of desert dust and sulphate over tropical Africa and the Atlantic Ocean region, *Atmos. Chem. Phys. Discuss.*, *5*, 5615–5644, doi:10.5194/acpd-5-5615-2005.

DeSouza-Machado, S. G., L. L. Strow, S. E. Hannon, and H. E. Motteler (2006), Infrared dust spectral signatures from AIRS, *Geophys. Res. Lett.*, *33*, L03801, doi:10.1029/2005GL024364.

Diner, D. J., J. V. Martonchik, R. A. Kahn, B. Pinty, N. Gobron, D. L. Nelson, and B. N. Holben (2005), Using angular and spectral shape similarity constraints to improve MISR aerosol and surface retrievals over land, *Remote Sens. Environ.*, *94*, 155–171, doi:10.1016/j.rse.2004.09.009.

Drobinski, P., B. Sultan, and S. Janicot (2005), Role of the Hoggar massif on the West African monsoon onset, *Geophys. Res. Lett.*, *32*, L01705, doi:10.1029/2004GL020710.

Dubief, J. (1979), Review of the North African climate with particular emphasis on the production of Eolian dust in the Sahel zone and in the Sahara, in *Saharan Dust*, edited by C. Morales, pp. 27–48, John Wiley, Chichester, U. K.

Dubovik, O., M. Herman, A. Holdak, T. Lapyonok, D. Tanré, J. L. Deuzé, F. Ducos, A. Sinyuk, and A. Lopatin (2011), Statistically optimized inversion algorithm for enhanced retrieval of aerosol properties from spectral multi-angle polarimetric satellite observations, *Atmos. Meas. Tech.*, *4*, 975–1018, doi:10.5194/amt-4-975-2011.

Dunion, J., and C. Velden (2004), The impact of the Saharan air layer on Atlantic tropical cyclone activity, *Bull. Am. Meteorol. Soc.*, *85*, 353–365, doi:10.1175/BAMS-85-3-353.

Emmel, C., P. Knippertz, and O. Schulz (2010), Climatology of convective density currents in the southern foothills of the Atlas Mountains, *J. Geophys. Res.*, *115*, D11115, doi:10.1029/2009JD012863.

Engelstaedter, S., and R. Washington (2007), Atmospheric controls on the annual cycle of North African dust, *J. Geophys. Res.*, *112*, D03103, doi:10.1029/2006JD007195.

Engelstaedter, S., and R. Washington (2008), Reply to comment by E. Williams on "Atmospheric controls on the annual cycle of North African dust," *J. Geophys. Res.*, *113*, D23110, doi:10.1029/2008JD010275.

Erickson, D. J., III, J. L. Hernandez, P. Ginoux, W. W. Gregg, C. McClain, and J. Christian (2003), Atmospheric iron delivery and surface ocean biological activity in the Southern Ocean and Patagonian region, *Geophys. Res. Lett.*, *30*(12), 1609, doi:10.1029/2003GL017241.

Evan, A. T., A. K. Heidinger, and M. J. Pavolonis (2006), Development of a new over-water advanced very high resolution radiometer dust detection algorithm, *Int. J. Remote Sens.*, *27*, 3903–3924, doi:10.1080/01431160600646359.

Farquharson, M. (1937), Haboobs and instability in the Sudan, *Q. J. R. Meteorol. Soc.*, *63*, 393–414, doi:10.1002/qj.49706327111.

Fasham, M. J. R. (2003), *Ocean Biogeochemistry*, Springer, Heidelberg, Germany.

Flamant, C., J.-P. Chaboureau, D. J. Parker, C. M. Taylor, J.-P. Cammas, O. Bock, F. Timouk, and J. Pelon (2007), Airborne observations of the impact of a convective system on the planetary boundary layer thermodynamics and aerosol distribution in the inter-tropical discontinuity region of the West African monsoon, *Q. J. R. Meteorol. Soc.*, *133*, 1175–1189, doi:10.1002/qj.97.

Formenti, P., L. Schütz, Y. Balkanski, K. Desboeufs, M. Ebert, K. Kandler, A. Petzold, D. Scheuvens, S. Weinbruch, and D. Zhang (2011), Recent progress in understanding physical and chemical properties of African and Asian mineral dust, *Atmos. Chem. Phys.*, *11*, 8231–8256, doi:10.5194/acp-11-8231-2011.

Forster, P., et al. (2007), Changes in atmospheric constituents and in radiative forcing, in *Climate Change 2007: The Physical Science Basis: Working Group I Contribution to the Fourth Assessment Report of the Intergovernmental Panel on Climate Change*, edited by S. Solomon et al., pp. 129–234, Cambridge Univ. Press, New York.

Freeman, M. (1952), *Duststorms of the Anglo-Egyptian Sudan*, *Meteorol. Rep. Ser.*, vol. 11, 22 pp., Her Majesty's Stn. Off., London.

Gamo, M. (1996), Thickness of the dry convection and large-scale subsidence above deserts, *Boundary Layer Meteorol.*, *79*(3), 265–278, doi:10.1007/BF00119441.

Ginoux, P., et al. (2001), Sources and distributions of dust aerosols simulated with the GOCART model, *J. Geophys. Res.*, *106*(D17), 20,255–20,273, doi:10.1029/2000JD000053.

Ginoux, P., D. Garbuzov, and N. C. Hsu (2010), Identification of anthropogenic and natural dust sources using Moderate Resolution Imaging Spectroradiometer (MODIS) Deep Blue level 2 data, *J. Geophys. Res.*, *115*, D05204, doi:10.1029/2009JD012398.

Grams, C. M., S. C. Jones, J. M. Marsham, D. J. Parker, J. M. Haywood, and V. Heuveline (2010), The Atlantic inflow to the Saharan heat low: Observations and modelling, *Q. J. R. Meteorol. Soc.*, *136*, 125–140, doi:10.1002/qj.429.

Grini, A., G. Myhre, C. S. Zender, and I. S. A. Isaksen (2005), Model simulations of dust sources and transport in the global atmosphere: Effects of soil erodibility and wind speed variability, *J. Geophys. Res.*, *110*, D02205, doi:10.1029/2004JD005037.

Hanna, S., and R. Yang (2001), Evaluations of mesoscale model's simulations of near-surface winds, temperature gradients, and mixing depths, *J. Appl. Meteorol.*, 40, 1095–1104, doi:10.1175/1520-0450(2001)040<1095:EOMMSO>2.0.CO;2.

Hannachi, A., A. Awad, and K. Ammar (2010), Climatology and classification of spring Saharan cyclone tracks, *Clim. Dyn.*, 37, 473–491, doi:10.1007/s00382-010-0941-9.

Haywood, J. M., P. N. Francis, M. D. Glew, and J. P. Taylor (2001), The optical properties and direct radiative effect of Saharan Dust: A case study of two Saharan dust outbreaks using aircraft data, *J. Geophys. Res.*, 106(D16), 18,417–18,430, doi:10.1029/2000JD900319.

Haywood, J. M., et al. (2008), Overview of the Dust and Biomass-burning Experiment and African Monsoon Multidisciplinary Analysis Special Observing Period-0, *J. Geophys. Res.*, 113, D00C17, doi:10.1029/2008JD010077.

Haywood, J. M., et al. (2011a), Motivation, rationale and key results from the GERBILS Saharan dust measurement campaign, *Q. J. R. Meteorol. Soc.*, 137, 1106–1116, doi:10.1002/qj.797.

Haywood, J. M., B. T. Johnson, S. R. Osborne, J. Mulcahy, M. E. Brooks, M. Harrison, S. F. Milton, and H. Brindley (2011b), Observations and modelling of the solar and terrestrial radiative effects of Saharan dust: A radiative closure case-study over oceans during the GERBILS campaign, *Q. J. R. Meteorol. Soc.*, 137, 1211–1226, doi:10.1002/qj.770.

Heintzenberg, J. (2009), The SAMUM-1 experiment over southern Morocco: Overview and introduction, *Tellus B*, 61, 2–11, doi:10.1111/j.1600-0889.2008.00403.x.

Herman, M., J. L. Deuzé, A. Marchand, B. Roger, and P. Lallart (2005), Aerosol remote sensing from POLDER/ADEOS over the ocean: Improved retrieval using a nonspherical particle model, *J. Geophys. Res.*, 110, D10S02, doi:10.1029/2004JD004798.

Holben, B. N., et al. (1998), AERONET—A federated instrument network and data archive for aerosol characterization, *Remote Sens. Environ.*, 66, 1–16, doi:10.1016/S0034-4257(98)00031-5.

Hollingsworth, A., et al. (2008), Toward a monitoring and forecasting system for atmospheric composition: The GEMS project, *Bull. Am. Meteorol. Soc.*, 89, 1147–1164, doi:10.1175/2008BAMS2355.1.

Houser, C. A., and W. G. Nickling (2001), The emission and vertical flux of particulate matter <10 μm from a disturbed clay-crusted surface, *Sedimentology*, 48, 255–267, doi:10.1046/j.1365-3091.2001.00359.x.

Hsu, N. C., S. C. Tsay, M. D. King, and J. R. Herman (2004), Aerosol properties over bright-reflecting source regions, *IEEE Trans. Geosci. Remote Sens.*, 42, 557–569, doi:10.1109/TGRS.2004.824067.

Hui, W. J., B. I. Cook, S. Ravi, J. D. Fuentes, and P. D'Odorico (2008), Dust-rainfall feedbacks in the West African Sahel, *Water Resour. Res.*, 44, W05202, doi:10.1029/2008WR006885.

Huneeus, N., et al. (2011), Global dust model intercomparison in AeroCom phase I, *Atmos. Chem. Phys.*, 11, 7781–7816, doi:10.5194/acp-11-7781-2011.

Husar, R. B., J. M. Prospero, and L. L. Stowe (1997), Characterization of tropospheric aerosols over the oceans with the NOAA advanced very high resolution radiometer optical thickness operational product, *J. Geophys. Res.*, 102, 16,889–16,909, doi:10.1029/96JD04009.

Idso, S., R. S. Ingram, and J. M. Pritchard (1972), An American haboob, *Bull. Am. Meteorol. Soc.*, 53, 930–935, doi:10.1175/1520-0477(1972)053<0930:AAH>2.0.CO;2.

Ishizuka, M., M. Mikami, J. F. Leys, Y. Yamada, S. Heidenreich, Y. Shao, and G. H. McTainsh (2008), Effects of soil moisture and dried raindroplet crust on saltation and dust emission, *J. Geophys. Res.*, 113, D24212, doi:10.1029/2008JD009955.

Jickells, T., et al. (2005), Global iron connections between desert dust, ocean biogeochemistry, and climate, *Science*, 308, 67–71, doi:10.1126/science.1105959.

Johnson, B. T., B. Heese, S. A. McFarlane, P. Chazette, A. Jones, and N. Bellouin (2008), Vertical distribution and radiative effects of mineral dust and biomass burning aerosol over West Africa during DABEX, *J. Geophys. Res.*, 113, D00C12, doi:10.1029/2008JD009848.

Kahn, R., et al. (2009), Desert dust aerosol air mass mapping in the western Sahara, using particle properties derived from space-based multi-angle imaging, *Tellus B*, 61, 239–251, doi:10.1111/j.1600-0889.2008.00398.x.

Kalashnikova, O. V., and R. A. Kahn (2008), Mineral dust plume evolution over the Atlantic from MISR and MODIS aerosol retrievals, *J. Geophys. Res.*, 113, D24204, doi:10.1029/2008JD010083.

Kanak, K. (2005), Numerical simulation of dust devil-scale vortices, *Q. J. R. Meteorol. Soc.*, 131, 1271–1292, doi:10.1256/qj.03.172.

Kandler, K., N. Benker, U. Bundke, E. Cuevas, M. Eberta, P. Knippertz, S. Rodríguez, L. Schütz, and S. Weinbruch (2007), Chemical composition and complex refractive index of Saharan mineral dust at Izaña, Tenerife (Spain) derived by electron microscopy, *Atmos. Environ.*, 41, 8058–8074, doi:10.1016/j.atmosenv.2007.06.047.

Kang, J.-Y., S.-C. Yoon, Y. Shao, and S.-W. Kim (2011), Comparison of vertical dust flux by implementing three dust emission schemes in WRF/Chem, *J. Geophys. Res.*, 116, D09202, doi:10.1029/2010JD014649.

Karyampudi, V. M., and T. N. Carlson (1988), Analysis and numerical simulations of the Saharan air layer and its effect on easterly wave disturbances, *J. Atmos. Sci.*, 45, 3102–3136, doi:10.1175/1520-0469(1988)045<3102:AANSOT>2.0.CO;2.

Kaufman, Y. J., I. Koren, and L. A. Remer (2005), The effect of smoke, dust, and pollution aerosol on shallow cloud development over the Atlantic Ocean, *Proc. Natl. Acad. Sci. U. S. A.*, 102, 11,207–11,212, doi:10.1073/pnas.0505191102.

Kittaka, C., D. M. Winker, M. A. Vaughan, A. Omar, and L. A. Remer (2011), Intercomparison of column aerosol optical depths from CALIPSO and MODIS-Aqua, *Atmos. Meas. Tech.*, 4, 131–141, doi:10.5194/amt-4-131-2011.

Klose, M., Y. Shao, M. K. Karremann, and A. H. Fink (2010), Sahel dust zone and synoptic background, *Geophys. Res. Lett.*, 37, L09802, doi:10.1029/2010GL042816.

Klüser, L., and T. Holzer-Popp (2010), Relationships between mineral dust and cloud properties in the West African Sahel, *Atmos. Chem. Phys.*, 10, 6901–6915, doi:10.5194/acp-10-6901-2010.

Klüser, L., D. Martynenko, and T. Holzer-Popp (2011), Thermal infrared remote sensing of mineral dust over land and ocean: A spectral SVD based retrieval approach for IASI, *Atmos. Meas. Tech.*, 4, 757–773, doi:10.5194/amt-4-757-2011.

Knippertz, P. (2007), Tropical-extratropical interactions related to upper-level troughs at low latitudes, *Dyn. Atmos. Oceans*, 43, 36–62, doi:10.1016/j.dynatmoce.2006.06.003.

Knippertz, P. (2008), Dust mobilization in the West African heat trough—The role of the diurnal cycle and of extratropical synoptic disturbances, *Meteorol. Z.*, 17, 553–563, doi:10.1127/0941-2948/2008/0315.

Knippertz, P., and A. H. Fink (2006), Synoptic and dynamic aspects of an extreme springtime Saharan dust outbreak, *Q. J. R. Meteorol. Soc.*, 132, 1153–1177, doi:10.1256/qj.05.109.

Knippertz, P., and M. C. Todd (2010), The central west Saharan dust hot spot and its relation to African easterly waves and extratropical disturbances, *J. Geophys. Res.*, 115, D12117, doi:10.1029/2009JD012819.

Knippertz, P., C. Deutscher, K. Kandler, T. Müller, O. Schulz, and L. Schütz (2007), Dust mobilization due to density currents in the Atlas region: Observations from the SAMUM 2006 field campaign, *J. Geophys. Res.*, 112, D21109, doi:10.1029/2007JD008774.

Knippertz, P., J. Trentmann, and A. Seifert (2009a), High-resolution simulations of convective cold pools over the

northwestern Sahara, *J. Geophys. Res.*, *114*, D08110, doi:10.1029/2008JD011271.

Knippertz, P., et al. (2009b), Dust mobilization and transport in the northern Sahara during SAMUM 2006—A meteorological overview, *Tellus B*, *61*, 12–31, doi:10.1111/j.1600-0889.2008.00380.x.

Knippertz, P., M. Tesche, B. Heinold, K. Kandler, C. Toledano, and M. Esselborn (2011), Dust mobilization and aerosol transport from West Africa to Cape Verde–A meteorological overview of SAMUM-2, *Tellus B*, *63*, 430–447, doi:10.1111/j.1600-0889.2011.00544.x.

Koch, J., and N. O. Renno (2005), The role of convective plumes and vortices on the global aerosol budget, *Geophys. Res. Lett.*, *32*, L18806, doi:10.1029/2005GL023420.

Kok, J. F. (2011), A scaling theory for the size distribution of emitted dust aerosols suggests climate models underestimate the size of the global dust cycle, *Proc. Natl. Acad. Sci. U. S. A.*, *108*, 1016–1021, doi:10.1073/pnas.1014798108.

Koren, I., and Y. J. Kaufman (2004), Direct wind measurements of Saharan dust events from Terra and Aqua satellites, *Geophys. Res. Lett.*, *31*, L06122, doi:10.1029/2003GL019338.

Koren, I., Y. J. Kaufman, R. Washington, M. C. Todd, Y. Rudich, V. J. Martins, and D. Rosenfeld (2006), The Bodélé depression—A single spot in the Sahara that provides most of the mineral dust to the Amazon forest, *Environ. Res. Lett.*, *1*, 014005, doi:10.1088/1748-9326/1/1/014005.

Krinner, G., O. Boucher, and Y. Balkanski (2006), Ice-free glacial northern Asia due to dust deposition on snow, *Clim. Dyn.*, *27*(6), 613–625, doi:10.1007/s00382-006-0159-z.

Lambert, F., B. Delmonte, J. R. Petit, M. Bigler, P. Kaufmann, M. Hutterli, T. F. Stocker, U. Ruth, J. P. Steffensen, and V. Maggi (2008), New constraints on the dust-climate couplings from the 800,000-year EPICA Dome C ice core, *Nature*, *452*, 616–619, doi:10.1038/nature06763.

Laurent, B., B. Marticorena, G. Bergametti, and F. Mei (2006), Modeling mineral dust emissions from Chinese and Mongolian deserts, *Global Planet. Change*, *52*, 121–141, doi:10.1016/j.gloplacha.2006.02.012.

Lawson, T. J. (1971), Haboob structure at Khartoum, *Weather*, *26*, 105–112.

Legrand, M., C. N'Doume, and I. Jankowiak (1994), Satellite-derived climatology of the Saharan aerosol, in *Passive Infrared Remote Sensing of Clouds and the Atmosphere II*, edited by D. K. Lynch, pp. 127–135, Soc. of Photo-Opt. Instrum. Eng., Bellingham, Wash.

Léon, J.-F., Y. Derimian, I. Chiapello, D. Tanré, T. Podvin, B. Chatenet, A. Diallo, and C. Deroo (2009), Aerosol vertical distribution and optical properties over M'Bour (16.96°W; 14.39°N), Senegal from 2006 to 2008, *Atmos. Chem. Phys.*, *9*, 9249–9261, doi:10.5194/acp-9-9249-2009.

Li, J., G. S. Okin, J. E. Herrick, J. Belnap, S. M. Munson, and M. E. Miller (2010), A simple method to estimate threshold friction velocity of wind erosion in the field, *Geophys. Res. Lett.*, *37*, L10402, doi:10.1029/2010GL043245.

Lu, H., and Y. Shao (1999), A new model for dust emission by saltation bombardment, *J. Geophys. Res.*, *104*, 16,827–16,842, doi:10.1029/1999JD900169.

Luo, C., N. M. Mahowald, and J. del Corral (2003), Sensitivity study of meteorological parameters on mineral aerosol mobilization, transport, and distribution, *J. Geophys. Res.*, *108*(D15), 4447, doi:10.1029/2003JD003483.

Maher, B. A., J. M. Prospero, D. Mackie, D. Gaiero, P. P. Hesse, and Y. Balkanski (2010), Global connections between aeolian dust, climate and ocean biogeochemistry at the present day and at the last glacial maximum, *Earth Sci. Rev.*, *99*, 61–97, doi:10.1016/j.earscirev.2009.12.001.

Mahowald, N. M., et al. (2010), Observed 20th century desert dust variability: Impact on climate and biogeochemistry, *Atmos.*

Chem. Phys., *10*, 10,875–10,893, doi:10.5194/acp-10-10875-2010.

Mahowald, N., K. Lindsay, D. Rothenberg, S. C. Doney, J. K. Moore, P. Thornton, J. T. Randerson, and C. D. Jones (2011), Desert dust and anthropogenic aerosol interactions in the Community Climate System Model coupled-carbon-climate model, *Biogeosciences*, *8*, 387–414, doi:10.5194/bg-8-387-2011.

Mallet, M., P. Tulet, D. Serça, F. Solmon, O. Dubovik, J. Pelon, V. Pont, and O. Thouron (2009), Impact of dust aerosols on the radiative budget, surface heat fluxes, heating rate profiles and convective activity over West Africa during March 2006, *Atmos. Chem. Phys.*, *9*, 7143–7160, doi:10.5194/acp-9-7143-2009.

Mangold, A., et al. (2011), Aerosol analysis and forecast in the European Centre for Medium-Range Weather Forecasts Integrated Forecast System: 3. Evaluation by means of case studies, *J. Geophys. Res.*, *116*, D03302, doi:10.1029/2010JD014864.

Marsham, J. H., D. J. Parker, C. M. Grams, C. M. Taylor, and J. M. Haywood (2008a), Uplift of Saharan dust south of the intertropical discontinuity, *J. Geophys. Res.*, *113*, D21102, doi:10.1029/2008JD009844.

Marsham, J. H., D. J. Parker, C. M. Grams, B. T. Johnson, W. M. F. Grey, and A. N. Ross (2008b), Observations of mesoscale and boundary-layer scale circulations affecting dust transport and uplift over the Sahara, *Atmos. Chem. Phys.*, *8*, 6979–6993, doi:10.5194/acp-8-6979-2008b.

Marsham, J. H., P. Knippertz, N. S. Dixon, D. J. Parker, and G. M. S. Lister (2011), The importance of the representation of deep convection for modeled dust-generating winds over West Africa during summer, *Geophys. Res. Lett.*, *38*, L16803, doi:10.1029/2011GL048368.

Marticorena, B., and G. Bergametti (1995), Modeling the atmospheric dust cycle: 1. Design of a soil-derived dust emission scheme, *J. Geophys. Res.*, *100*(D8), 16,415–16,430, doi:10.1029/95JD00690.

Marticorena, B., B. Chatenet, J. L. Rajot, S. Traoré, M. Coulibaly, A. Diallo, I. Koné, A. Maman, T. N. Diaye, and A. Zakou (2010), Temporal variability of mineral dust concentrations over West Africa: Analyses of a pluriannual monitoring from the AMMA Sahelian Dust Transect, *Atmos. Chem. Phys.*, *10*, 8899–8915, doi:10.5194/acp-10-8899-2010.

McConnell, C. L., E. J. Highwood, H. Coe, P. Formenti, B. Anderson, S. Osborne, S. Nava, K. Desboeufs, G. Chen, and M. A. J. Harrison (2008), Seasonal variations of the physical and optical characteristics of Saharan dust: Results from the Dust Outflow and Deposition to the Ocean (DODO) experiment, *J. Geophys. Res.*, *113*, D14S05, doi:10.1029/2007JD009606.

McTainsh, G. H. (1999), Dust transport and deposition, in *Aeolian Environments, Sediments and Landforms*, edited by A. S. Goudie, I. Livingstone, and S. Stokes, chap. 9, pp. 181–211, John Wiley, Chichester, U. K.

Membery, D. (1985), A gravity-wave haboob?, *Weather*, *40*, 214–221.

Menut, L. (2008), Sensitivity of hourly Saharan dust emissions to NCEP and ECMWF modeled wind speed, *J. Geophys. Res.*, *113*, D16201, doi:10.1029/2007JD009522.

Menut, L., I. Chiapello, and C. Moulin (2009), Predictability of mineral dust concentrations: The African Monsoon Multidisciplinary Analysis first short observation period forecasted with CHIMERE-DUST, *J. Geophys. Res.*, *114*, D07202, doi:10.1029/2008JD010523.

Michel, A. E., C. R. Usher, and V. H. Grassian (2003), Reactive uptake of ozone on mineral oxides and mineral dusts, *Atmos. Environ.*, *37*, 3201–3211, doi:10.1016/S1352-2310(03)00319-4.

Miller, S. S. D., A. P. Kuciauskas, M. Liu, Q. Ji, J. S. Reid, D. W. Breed, A. L. Walker, and A. A. Mandoos (2008), Haboob dust storms of the southern Arabian Peninsula, *J. Geophys. Res.*, *113*, D01202, doi:10.1029/2007JD008550.

Min, Q.-L., R. Li, B. Lin, E. Joseph, S. Wang, Y. Hu, V. Morris, and F. Chang (2009), Evidence of mineral dust altering

cloud microphysics and precipitation, *Atmos. Chem. Phys.*, *9*, 3223–3231, doi:10.5194/acp-9-3223-2009.

Mishchenko, M. I., I. V. Geogdzhayev, B. Cairns, B. E. Carlson, J. Chowdhary, A. A. Lacis, L. Liu, W. B. Rossow, and L. D. Travis (2007), Past, present, and future of global aerosol climatologies derived from satellite observations: A perspective, *J. Quant. Spectrosc. Radiat. Transfer*, *106*, 325–347, doi:10.1016/j.jqsrt.2007.01.007.

Mishchenko, M. I., L. Liu, L. D. Travis, B. Cairns, and A. A. Lacis (2010), Toward unified satellite climatology of aerosol properties: Part 3. MODIS versus MISR versus AERONET, *J. Quant. Spectrosc. Radiat. Transfer*, *111*, 540–552, doi:10.1016/j.jqsrt.2009.11.003.

Molesworth, A. M., L. E. Cuevas, A. P. Morse, J. R. Herman, and M. C. Thomson (2002), Correspondence: Dust clouds and spread of infection, *Lancet*, *359*, 81–82, doi:10.1016/S0140-6736(02)07304-X.

Morcrette, J.-J., A. Beljaars, A. Benedetti, L. Jones, and O. Boucher (2008), Sea-salt and dust aerosols in the ECMWF IFS model, *Geophys. Res. Lett.*, *35*, L24813, doi:10.1029/2008GL036041.

Mulitza, S., et al. (2010), Increase in African dust flux at the onset of commercial agriculture in the Sahel region, *Nature*, *466*, 226–228, doi:10.1038/nature09213.

Nickovic, S., A. Papadopoulos, O. Kakaliagou, and G. Kallos (2001), Model for prediciton of desert dust cycle in the atmosphere, *J. Geophys. Res.*, *106*, 18,113–18,129, doi:10.1029/2000JD900794.

N'Tchayi Mbourou, G., J. J. Bertrand, and S. E. Nicholson (1997), The diurnal and seasonal cycles of wind-borne dust over Africa north of the equator, *J. Appl. Meteorol.*, *36*, 868–882, doi:10.1175/1520-0450(1997)036<0868:TDASCO>2.0.CO;2.

Ohno, H., and T. Takemi (2010), Mechanisms for intensification and maintenance of numerically simulated dust devils, *Atmos. Sci. Lett.*, *11*, 27–32.

Okin, G. S. (2008), A new model of wind erosion in the presence of vegetation, *J. Geophys. Res.*, *113*, F02S10, doi:10.1029/2007JF000758.

Okin, G. S., N. Mahowald, O. A. Chadwick, and P. Artaxo (2004), Impact of desert dust on the biogeochemistry of phosphorus in terrestrial ecosystems, *Global Biogeochem. Cycles*, *18*, GB2005, doi:10.1029/2003GB002145.

Painter, T. H., A. P. Barrett, C. C. Landry, J. C. Neff, M. P. Cassidy, C. R. Lawrence, K. E. McBride, and G. L. Farmer (2007), Impact of disturbed desert soils on duration of mountain snow cover, *Geophys. Res. Lett.*, *34*, L12502, doi:10.1029/2007GL030284.

Parker, D. J., R. R. Burton, A. Diongue-Niang, R. J. Ellis, M. Felton, C. M. Taylor, C. D. Thorncroft, P. Bessemoulin, and A. M. Tompkins (2005), The diurnal cycle of the West African monsoon circulation, *Q. J. R. Meteorol. Soc.*, *131*, 2839–2860, doi:10.1256/qj.04.52.

Pérez, C., S. Nickovic, G. Pejanovic, J. M. Baldasano, and E. Özsoy (2006), Interactive dust-radiation modeling: A step to improve weather forecasts, *J. Geophys. Res.*, *111*, D16206, doi:10.1029/2005JD006717.

Peyridieu, S., A. Chédin, D. Tanré, V. Capelle, C. Pierangelo, N. Lamquin, and R. Armante (2010), Saharan dust infrared optical depth and altitude retrieved from AIRS: A focus over North Atlantic—Comparison to MODIS and CALIPSO, *Atmos. Chem. Phys.*, *10*, 1953–1967, doi:10.5194/acp-10-1953-2010.

Peyrillé, P., J.-P. Lafore, and J.-L. Redelsperger (2007), An idealized two-dimensional framework to study the West African monsoon. Part I: Validation and key controlling factors, *J. Atmos. Sci.*, *64*, 2765–2782, doi:10.1175/JAS3919.1.

Pierangelo, C., A. Chédin, S. Heilliette, N. Jacquinet-Husson, and R. Armante (2004), Dust altitude and infrared optical depth from AIRS, *Atmos. Chem. Phys.*, *4*, 1813–1822, doi:10.5194/acp-4-1813-2004.

Poulsen, C. A., R. Siddans, G. E. Thomas, A. Sayer, R. G. Grainger, O. Perez-Navarro, O. Portela-Arjona, and P.-Y. Deschamps

(2009), ESA GlobAerosol: Final validation and intercomparison report, version 3.2, report, Eur. Space Agency, Paris. [Available at http://www.globaerosol.info/docs/globaer_fvir_v3p2.pdf.]

Prospero, J. M., and T. N. Carlson (1972), Vertical and areal distributions of Saharan dust over the western equatorial North Atlantic Ocean, *J. Geophys. Res.*, *77*, 5255–5265, doi:10.1029/JC077i027p05255.

Prospero, J. M., P. Ginoux, O. Torres, S. Nicholson, and T. Gill (2002), Environmental characterization of global sources of atmospheric soil dust identified with the NIMBUS7 Total Ozone Mapping Spectrometer (TOMS) absorbing aerosol product, *Rev. Geophys.*, *40*(1), 1002, doi:10.1029/2000RG000095.

Raasch, S., and T. Franke (2011), Structure and formation of dust devil-like vortices in the atmospheric boundary layer: A high-resolution numerical study, *J. Geophys. Res.*, *116*, D16120, doi:10.1029/2011JD016010.

Rajot, J. L., et al. (2008), AMMA dust experiment: An overview of measurements during the dry season special observation period (SOP0) at the Banizoumbou (Niger) supersite, *J. Geophys. Res.*, *113*, D00C14, doi:10.1029/2008JD009906.

Ramon, D., and R. Santer (2001), Operational remote sensing of aerosols over land to account for directional effects, *Appl. Opt.*, *40*, 3060–3075, doi:10.1364/AO.40.003060.

Redelsperger, J. L., C. D. Thorncroft, A. Diedhiou, T. Lebel, D. J. Parker, and J. Polcher (2006), African monsoon multidisciplinary analysis—An international research project and field campaign, *Bull. Am. Meteorol. Soc.*, *87*, 1739–1746, doi:10.1175/BAMS-87-12-1739.

Reinfried, F., I. Tegen, B. Heinold, O. Hellmuth, K. Schepanski, U. Cubasch, H. Hübener, and P. Knippertz (2009), Density currents in the Atlas Region leading to dust mobilization: A model sensitivity study, *J. Geophys. Res.*, *114*, D08127, doi:10.1029/2008JD010844.

Remer, L. A., et al. (2005), The MODIS aerosol algorithm, products and validation, *J. Atmos. Sci.*, *62*, 947–973, doi:10.1175/JAS3385.1.

Rennó, N. O., M. L. Burkett, and M. P. Larkin (1998), A simple thermodynamical theory for dust devils, *J. Atmos. Sci.*, *55*, 3244–3252, doi:10.1175/1520-0469(1998)055<3244:ASTTFD>2.0.CO;2.

Richardson, M., et al. (2007), Measurements of heterogeneous ice nuclei in the western United States in springtime and their relation to aerosol characteristics, *J. Geophys. Res.*, *112*, D02209, doi:10.1029/2006JD007500.

Rodwell, M. J., and T. Jung (2008), Understanding the local and global impacts of model physics changes: An aerosol example, *Q. J. R. Meteorol. Soc.*, *134*, 1479–1497, doi:10.1002/qj.298.

Rosenfeld, D., Y. Rudich, and R. Lahav (2001), Desert dust suppressing precipitation: A possible desertification feedback loop, *Proc. Natl. Acad. Sci. U. S. A.*, *98*, 5975–5980, doi:10.1073/pnas.101122798.

Roskovensky, J. K., and K. N. Liou (2005), Differentiating airborne dust from cirrus clouds using MODIS data, *Geophys. Res. Lett.*, *32*, L12809, doi:10.1029/2005GL022798.

Sander, N., and S. C. Jones (2008), Diagnostic measures for assessing numerical forecasts of African easterly waves, *Meteorol. Z.*, *17*, 209–220, doi:10.1127/0941-2948/2008/0269.

Schepanski, K., and P. Knippertz (2011), Soudano-Saharan depressions and their importance for precipitation and dust: A new perspective on a classical synoptic concept, *Q. J. R. Meteorol. Soc.*, *137*, 1431–1445, doi:10.1002/qj.850.

Schepanski, K., I. Tegen, B. Laurent, B. Heinold, and A. Macke (2007), A new Saharan dust source activation frequency map derived from MSG-SEVIRI IR-channels, *Geophys. Res. Lett.*, *34*, L18803, doi:10.1029/2007GL030168.

Schepanski, K., I. Tegen, M. C. Todd, B. Heinold, G. Bönisch, B. Laurent, and A. Macke (2009), Meteorological processes forcing Saharan dust emission inferred from MSG-SEVIRI observations of subdaily dust source activation and numerical

models, *J. Geophys. Res.*, *114*, D10201, doi:10.1029/2008JD010325.

Schulz, M., M. Chin, and S. Kinne (2009), The Aerosol Model Comparison Project, AeroCom, Phase II: Clearing up diversity, *IGAC Newsl.*, *41*, 2–11.

Schutz, B. E., H. J. Zwally, C. A. Shuman, D. Hancock, and J. P. DiMarzio (2005), Overview of the ICESat Mission, *Geophys. Res. Lett.*, *32*, L21S01, doi:10.1029/2005GL024009.

Shao, Y. (2004), Simplification of a dust emission scheme and comparison with data, *J. Geophys. Res.*, *109*, D10202, doi:10.1029/2003JD004372.

Shao, Y., and M. Mikami (2005), Heterogeneous saltation: Theory, observation and comparison, *Boundary Layer Meteorol.*, *115*, 359–379, doi:10.1007/s10546-004-7089-2.

Shao, Y., M. R. Raupach, and J. F. Leys (1996), A model for predicting aeolian sand drift and dust entrainment on scales from paddock to region, *Aust. J. Soil Res.*, *34*, 309–342, doi:10.1071/SR9960309.

Shao, Y., A. H. Fink, and M. Klose (2010), Numerical simulation of a continental-scale Saharan dust event, *J. Geophys. Res.*, *115*, D13205, doi:10.1029/2009JD012678.

Shao, Y., K.-H. Wyrwoll, A. Chappell, J. Huang, Z. Lin, G. H. McTainsh, M. Mikami, T. Y. Tanaka, X. Wang, and S. Yoon (2011), Dust cycle: An emerging core theme in Earth system science, *Aeolian Res.*, *2*(4), 181–204, doi:10.1016/j.aeolia.2011.02.001.

Shen, B.-W., W.-K. Tao, and M.-L. C. Wu (2010), African easterly waves in 30-day high-resolution global simulations: A case study during the 2006 NAMMA period, *Geophys. Res. Lett.*, *37*, L18803, doi:10.1029/2010GL044355.

Sima, A., D. D. Rousseau, M. Kageyama, G. Ramstein, M. Schulz, Y. Balkanski, A. Antoine, F. Dulac, and C. Hatte (2009), Imprint of North-Atlantic millennial-timescale variability on western European loess deposits as viewed in a dust emission model, *Quat. Sci. Rev.*, *28*, 2851–2866, doi:10.1016/j.quascirev.2009.07.016.

Sinclair, P. (1969), General characteristics of dust devils, *J. Appl. Meteorol.*, *8*, 32–45, doi:10.1175/1520-0450(1969)008<0032:GCODD>2.0.CO;2.

Slingo, A., et al. (2006), Observations of the impact of a major Saharan dust storm on the atmospheric radiation balance, *Geophys. Res. Lett.*, *33*, L24817, doi:10.1029/2006GL027869.

Solmon, F., M. Mallet, N. Elguindi, F. Giorgi, A. Zakey, and A. Konaré (2008), Dust aerosol impact on regional precipitation over western Africa, mechanisms and sensitivity to absorption properties, *Geophys. Res. Lett.*, *35*, L24705, doi:10.1029/2008GL035900.

Solomos, S., G. Kallos, J. Kushta, M. Astitha, C. Tremback, A. Nenes, and Z. Levin (2011), An integrated modeling study on the effects of mineral dust and sea salt particles on clouds and precipitation, *Atmos. Chem. Phys.*, *11*, 873–892, doi:10.5194/acp-11-873-2011.

Spinhirne, J. D., S. P. Palm, W. D. Hart, D. L. Hlavka, and E. J. Welton (2005), Cloud and aerosol measurements from GLAS: Overview and initial results, *Geophys. Res. Lett.*, *32*, L22S03, doi:10.1029/2005GL023507.

Spracklen, D. V., K. J. Pringle, K. S. Carslaw, M. P. Chipperfield, and G. W. Mann (2005), A global off-line model of size-resolved aerosol microphysics: Part I. Model development and prediction of aerosol properties, *Atmos. Chem. Phys.*, *5*, 2227–2252, doi:10.5194/acp-5-2227-2005.

Stanelle, T., B. Vogel, H. Vogel, D. Bäumer, and C. Kottmeier (2010), Feedback between dust particles and atmospheric processes over West Africa during dust episodes in March 2006 and June 2007, *Atmos. Chem. Phys.*, *10*, 10,771–10,788, doi:10.5194/acp-10-10771-2010.

Stuut, J.-B., I. Smalley, and K. O'Hara Dhandt (2009), Aeolian dust in Europe: African sources and European deposits, *Quat. Int.*, *198*, 234–245, doi:10.1016/j.quaint.2008.10.007.

Sullivan, P. P., and E. G. Patton (2011), The effect of mesh resolution on convective boundary layer statistics and structures generated by large-eddy simulation, *J. Atmos. Sci.*, *68*, 2395–2415, doi:10.1175/JAS-D-10-05010.1.

Sutton, L. J. (1925), Haboobs, *Q. J. R. Meteorol. Soc.*, *51*, 25–30, doi:10.1002/qj.49705121305.

Swap, R., M. Garstang, S. Greco, R. Talbot, and P. Kållberg (1992), Saharan dust in the Amazon basin, *Tellus B*, *44*, 133–149, doi:10.1034/j.1600-0889.1992.t01-1-00005.x.

Takemi, T. (2005), Explicit simulations of convective-scale transport of mineral dust in severe convective weather, *J. Meteorol. Soc. Jpn.*, *83A*, 187–203, doi:10.2151/jmsj.83A.187.

Tanré, D. (2010), Derivation of tropospheric aerosol properties from satellite observations, *C. R. Geosci.*, *342*, 403–411, doi:10.1016/j.crte.2010.02.003.

Taylor, C. M., A. Gounou, F. Guichard, P. H. Harris, R. J. Ellis, F. Couvreux, and M. DeKauwe (2011), Frequency of Sahelian storm initiation enhanced over mesoscale soil-moisture patterns, *Nat. Geosci.*, *4*, 430–433, doi:10.1038/ngeo1173.

Tegen, I., and K. Schepanski (2009), The global distribution of dust, *IOP Conf. Ser. Earth Env. Sci.*, *7*, 012001, doi:10.1088/1755-1307/7/1/012001.

Tesche, M., et al. (2009), Vertical profiling of Saharan dust with Raman lidars and airborne HSRL during SAMUM, *Tellus B*, *61*, 144–164, doi:10.1111/j.1600-0889.2008.00390.x.

Textor, C., et al. (2006), Analysis and quantification of the diversities of aerosol life cycles within AeroCom, *Atmos. Chem. Phys.*, *6*, 1777–1813, doi:10.5194/acp-6-1777-2006.

Textor, C., et al. (2007), The effect of harmonized emissions on aerosol properties in global models—An AeroCom experiment, *Atmos. Chem. Phys.*, *7*, 4489–4501, doi:10.5194/acp-7-4489-2007.

Thomas, G. E., C. A. Poulsen, R. L. Curier, G. De Lewuw, S. H. Marsh, E. Carboni, R. G. Grainger, and R. Siddans (2007), Comparison of AATSR and SEVIRI aerosol retrievals over the Northern Adriatic, *Q. J. R. Meteorol. Soc.*, *133*, 85–95, doi:10.1002/qj.126.

Thomas, G. E., C. A. Poulsen, A. M. Sayer, S. H. Marsh, S. M. Dean, E. Carboni, R. Siddans, R. G. Grainger, and B. N. Lawrence (2009), The GRAPE aerosol retrieval algorithm, *Atmos. Meas. Tech.*, *2*, 679–701, doi:10.5194/amt-2-679-2009.

Timmreck, C., and M. Schulz (2004), Significant dust simulation differences in nudged and climatological operation mode of the AGCM ECHAM, *J. Geophys. Res.*, *109*, D13202, doi:10.1029/2003JD004381.

Todd, M. C., V. Martins, R. Washington, G. Lizcano, O. Dubovik, S. M'Bainayel, and S. Engelstaedter (2007), Mineral dust emission from the Bodélé Depression, Chad during BoDEx 2005, *J. Geophys. Res.*, *112*, D06207, doi:10.1029/2006JD007170.

Todd, M. C., et al. (2008a), Quantifying uncertainty in estimates of mineral dust flux: An intercomparison of model performance over the Bodélé Depression, northern Chad, *J. Geophys. Res.*, *113*, D24107, doi:10.1029/2008JD010476.

Todd, M. C., R. Washington, S. Raghavan, G. Lizcano, and P. Knippertz (2008b), Regional model simulations of the Bodélé low-level jet of northern Chad during the Bodélé Dust Experiment (BoDEx 2005), *J. Clim.*, *21*, 995–1012, doi:10.1175/2007JCLI1766.1.

Tompkins, A. M., C. Cardinali, J.-J. Morcrette, and M. Rodwell (2005), Influence of aerosol climatology on forecasts of the African Easterly Jet, *Geophys. Res. Lett.*, *32*, L10801, doi:10.1029/2004GL022189.

Torres, O., P. K. Bhartia, J. R. Herman, Z. Ahmad, and J. Gleason (1998), Derivation of aerosol properties from satellite measurements of backscattered ultraviolet radiation: Theoretical basis, *J. Geophys. Res.*, *103*(D14), 17,099–17,110, doi:10.1029/98JD00900.

Tulet, P., M. Mallet, V. Pont, J. Pelon, and A. Boone (2008), The 7–13 March 2006 dust storm over West Africa: Generation,

transport, and vertical stratification, *J. Geophys. Res.*, *113*, D00C08, doi:10.1029/2008JD009871.

Uno, I., et al. (2006), Dust model intercomparison (DMIP) study over Asia: Overview, *J. Geophys. Res.*, *111*, D12213, doi:10.1029/2005JD006575.

Van de Wiel, B. J. H., A. F. Moene, G. J. Steeneveld, P. Baas, F. C. Bosveld, and A. A. M. Holtslag (2010), A conceptual view on inertial oscillations and nocturnal low-level jets, *J. Atmos. Sci.*, *67*, 2679–2689, doi:10.1175/2010JAS3289.1.

Wakimoto, R. M. (2001), Convectively driven high wind events, in *Severe Convective Storms*, *Meteorol. Monogr. Ser.*, vol. 28, edited by C. A. Doswell III, pp. 255–298, Am. Meteorol. Soc., Boston.

Warren, S., and W. Wiscombe (1980), A model for the spectral albedo of snow. Part II: Snow containing atmospheric aerosols, *J. Atmos. Sci.*, *37*, 2734–2745, doi:10.1175/1520-0469(1980) 037<2734:AMFTSA>2.0.CO;2.

Washington, R., and M. C. Todd (2005), Atmospheric controls on mineral dust emission from the Bodélé Depression, Chad: The role of the low level jet, *Geophys. Res. Lett.*, *32*, L17701, doi:10.1029/2005GL023597.

Washington, R., M. C. Todd, A. S. Goudie, and N. Middleton (2003), Global dust storm source areas determined by the total ozone monitoring spectrometer and ground observations, *Ann. Assoc. Am. Geogr.*, *93*, 297–313, doi:10.1111/1467-8306. 9302003.

Washington, R., M. C. Todd, S. Engelstaedter, S. Mbainayel, and F. Mitchell (2006), Dust and the low-level circulation over the Bodélé Depression, Chad: Observations from BoDEx 2005, *J. Geophys. Res.*, *111*, D03201, doi:10.1029/2005JD006502.

Westphal, D., O. Toon, and T. Carlson (1988), A case study of mobilization and transport of Saharan dust, *J. Atmos. Sci.*, *45*, 2145–2175, doi:10.1175/1520-0469(1988)045<2145: ACSOMA>2.0.CO;2.

Williams, E. (2008), Comment on "Atmospheric controls on the annual cycle of North African dust" by S. Engelstaedter and R. Washington, *J. Geophys. Res.*, *113*, D23109, doi:10.1029/ 2008JD009930.

Williams, E., N. Nathou, E. Hicks, C. Pontikis, B. Russell, M. Miller, and M. Bartholomew (2008), The electrification of dust-lofting gust fronts ('haboobs') in the Sahel, *Atmos. Res.*, *91*, 292–298, doi:10.1016/j.atmosres.2008.05.017.

Winckler, G., R. F. Anderson, M. Q. Fleisher, D. McGee, and N. Mahowald (2008), Covariant glacial-interglacial dust fluxes in the equatorial Pacific and Antarctica, *Science*, *320*, 93–96, doi:10.1126/science.1150595.

Winker, D. M., M. A. Vaughan, A. Omar, Y. Hu, K. A. Powell, Z. Liu, W. H. Hunt, and S. A. Young (2009), Overview of the CALIPSO Mission and CALIOP data processing algorithms, *J. Atmos. Oceanic Technol.*, *26*, 2310–2323, doi:10.1175/ 2009JTECHA1281.1.

Yoshioka, M., N. M. Mahowald, A. J. Conley, W. D. Collins, D. W. Fillmore, C. S. Zender, and D. B. Coleman (2007), Impact of desert dust radiative forcing on Sahel precipitation: Relative importance of dust compared to sea surface temperature variations, vegetation changes, and greenhouse gas warming, *J. Clim.*, *20*, 1445–1467, doi:10.1175/JCLI4056.1.

Zender, C. S., R. L. Miller, and I. Tegen (2004), Quantifying mineral dust mass budgets: Terminology, constraints, and current estimates, *Eos Trans. AGU*, *85*(48), 509,512, doi:10.1029/ 2004EO480002.

Zhang, D.-L., and W.-Z. Zheng (2004), Diurnal cycles of surface winds and temperatures as simulated by five boundary layer parameterizations, *J. Appl. Meteorol.*, *43*, 157–169, doi:10.1175/ 1520-0450(2004)043<0157:DCOSWA>2.0.CO;2.

Zhong, S., and J. D. Fast (2003), An evaluation of MM5, RAMS, and Meso Eta at sub-kilometer resolution using the VTMX field campaign data in the Salt Lake Valley, *Mon. Weather Rev.*, *131*, 1301–1322, doi:10.1175/1520-0493(2003) 131<1301:AEOTMR>2.0.CO;2.

P. Knippertz, School of Earth and Environment, University of Leeds, Leeds LS2 9JT, UK. (p.knippertz@leeds.ac.uk)

M. C. Todd, Department of Geography, University of Sussex, Brighton BN1 9RH, UK.